FIU FLORIDA INTERNATIONAL UNIVERSITY

# Design and implementation of dye-tracer injection test, Cudjoe Key, Florida Keys.

FINAL REPORT

Submitted to:

CH2M Hills on behalf of
Florida Keys Aqueduct Authority
Attention: **Tom. G. Walker, PE, BCEE**
Deputy Executive Director
Utility Operations Division
Florida Keys Aqueduct Authority
and
Andrew Smyth
CH2M Hill

**Henry O. Briceño, Reinaldo Garcia, Piero Gardinali**
**Kevin Boswell, Alexandra Serna**
Florida International University
and
**Eugene Shinn**
University of South Florida

April 11th, 2014

# EXECUTIVE SUMMARY

Monroe County and the Florida Keys Aqueduct Authority (FKAA) are currently constructing the Regional Centralized Wastewater Collection System and the Advanced Treatment Wastewater Facility (AWTF) located at Cudjoe Key, where treated waters would be disposed by injection through four Class V shallow wells (120 ft). There are reports documenting the occurrence of impervious layers within the rock pile that might preclude vertical flow of ground waters to the surface. Likewise, there is abundant information documenting high hydraulic conductivity from shallow wells to surface waters elsewhere in the Florida Keys. Facing this duality and controversial technical information, and to guarantee that water quality in the ecosystems surrounding AWTF are not impacted by the injection operations, the FKAA requested from Florida International University (FIU) the design and implementation of a dye-tracer injection test.

The final objective of this test was to either confirm or rule-out the existence of hydraulic connection between the shallow injection wells discharge and surface waters. The design of the test was performed with the Environmental Protection Agency's **EHDT** software to estimate tracer mass, sampling frequencies and dye breakthrough curves for selected monitoring distances. Test monitoring samples were collected at 2 injection wells (IW) and 4 observation wells (OW), and along transects in surface water bodies as recommended by the modeled design and the photogeological interpretation of satellite and Lidar images.

Execution of the project consisted of four phases, 1) Modeling; 2) Baseline Characterization; 3) Freshwater Injection; and 4) Dye Injection. During phases 2 to 4 exhaustive monitoring was performed. We conclude that there are convincing evidences that injected freshwater at the current injection depth of 80' to 120', and at the experimental injection rate of 420 gal/min, readily migrates upward and then laterally to the unconfined shallow aquifer and eventually to surface waters. These results are similar to those found by other researchers elsewhere in the Florida Keys.

## TABLE OF CONTENTS


| | |
|---|---|
| Executive Summary | 2 |
| Introduction | 4 |
| Objective | 5 |
| Development of Geological Model | 5 |
| Photogeological Interpretation | 6 |
| Regional Stratigraphy to Local Geology | 11 |
| Dye-tracer Injection Test Design | 14 |
| Efficient Hydrologic Tracer-Test Design (EHTD) Program | 14 |
| Baseline Study | 21 |
| Freshwater Injection | 27 |
| Dye-tracer Injection | 30 |
| Results of dye-tracer Injection | 30 |
| Conclusion | 38 |
| REFERENCES | 39 |
| APPENDIX 1: Data Summary Report | 42 |

# Introduction

The Florida Keys National Marine Sanctuary contains nationally significant marine environments such as mangrove forest, large seagrass beds, and the only living coral barrier reef in North America. The economy of Monroe County is based upon tourism, and millions of people visit the Florida Keys every year, mostly because of these natural wonders and especially the reefs, whose estimated asset value is of $7.6 billion (Johns et al., 2001).

Monroe County is devoting especial effort and funds to curtail pollution to the Sanctuary from runoff and canals, and in conjunction with the Florida Keys Aqueduct Authority (FKAA), is incorporating communities to the Regional Centralized Wastewater Collection System and Advanced Treatment Wastewater Facility. The proposed Wastewater Treatment Facility (AWTF), located in Cudjoe Key, will use an advanced, five-stage Bardenpho Wastewater Treatment System to provide service to Lower Sugarloaf Key, Upper Sugarloaf Key, Cudjoe Key, Summerland Key, Ramrod Key, Little Torch Key and Big Pine Key (Fig 1), to confront and solve the most important source of pollution from these keys, human waste.

We subdivided the study into three main phases, Baseline characterization (Feb 17$^{th}$ – Feb 25$^{th}$), Freshwater Injection test (Feb 27$^{th}$ – 30$^{th}$) and dye-tracer Injection test (March 5$^{th}$ to March 26$^{th}$).

# Objective

In order to guarantee that injected treated waters do not reach the surface and pollute further the valuable water bodies and ecosystem of the Florida Keys National Marine Sanctuary, the FKAA requested from Florida International University (FIU) the design and implementation of a dye-tracer injection test. The objective of the test was to either confirm or to rule-out the existence of hydraulic connection between the shallow injection wells discharge and surface waters in Cudjoe Key.

# Development of Underground Geological Model

Injection dye-trace tests require a reference framework of the test site underground geology, but Cudjoe Key had not been the specific subject of geological cartography in the past, and most of the available information came from regional studies (Hoffmeister and Multer 1968; Cunningham et al. 1998). A detailed discussion of available geologic information was provided in the proposal for this project, so here we will only cherry-pick that information of significant value for our purpose. Knowing that rocks of the Florida Keys have suffered intense karst processes in the last million years driven by climate and sea level fluctuations (White, 1970; Brinkmann and Reeder, 1994; Tihansky, 1999; Shinn et al. 1999a), our first attempt to assemble an underground geologic model for Cudjoe Key was by tapping on the existing geological literature, especially related to karst development.

Karsting of carbonate rocks in the Florida Keys have rendered highly transmissive and heterogeneous zones within the carbonate aquifers (Shinn 1999a, 1999b; Paul et al. 1995, 1997; Reich et al. 2001), with flow rates ranging from 1 to tens of m/day. On the other hand, Böhlke et al. (1999) and Reich et a.l (2001) studied ground water underlying both, the Florida Bay and the Atlantic coast side of the Keys and found that recent fine sediments on top of the bedrock are the most efficient barriers to groundwater migration to the surface. Coniglio et al. (1983a, 1983b) identified the existence of at least five regional caliche intervals within the Key Largo Limestone which behave as “impermeable barrier to upward groundwater flow”.

# Photogeological Interpretation

Groundwater flow in carbonate terrains like that of Cudjoe Key is in many instances controlled by rock fracturing (joints, faults), bedding planes or stratigraphy. In areas like the Florida Keys, where bedding is mostly horizontal rocks close to surface have suffered intense karsting, solution features and/or dense fracturing control shallow aquifer behavior. At depth, below the epikarst, fracturing density (frequency) diminishes but fractures tend to be larger and wider. Generally deep fractures are related to large regional scale fracture patterns of tectonic origin.

The existence of fracture systems in rocks of Cudjoe Key or the Lower Keys have not been assessed before, but their presence may be suggested by the development of linear features which, in turn, may be observed by remote sensing methods. Also, regional fracture systems are indicative of deep fractures extending hundreds of meters deep. Likewise, the occurrence of epikarst features, such as sinkholes and

intense fracturing, may be identified in satellite images and aerial photographs and verified in the field. We have attempted a rapid and preliminary photogeological interpretation of Lidar and satellite images (Google Earth images) of Cudjoe Key for linear features and for circular features as potential indicators of planar discontinuities and perhaps collapse structures (sinkholes) respectively. In order to validate the interpretations we explored the site on foot and performed ground-truthing of location and nature of interpreted features.

First we simply delineated persistent regional linear features as seen in satellite images of the Lower Keys (i.e. channels, shoreline, vegetation pattern contacts and other aligned geomorphic features). In a first approach, we presumed those linear features represent the surface expression of deep fractures (Fig 1). We performed similar observations on Cudjoe Key itself and delineated many features with the same orientation as those found at regional scale (Fig 2). The scientific rationale behind these interpretations is that some of these features, if existing and extending at depth to the injection zone (deeper that 80 ft) may connect surface and injected waters, becoming expedite routes to injected waters to reach surface water bodies.

We have also identified linear and circular features in satellite and Lidar images of Cudjoe Key (Fig 3) which could be surficial expression of rock solution processes and the development of sinkholes. Finally, we mapped diverse features (linear, circular and irregular) on satellite images of the study site (Fig 4 ) which are extremely common in Cudjoe Key, suggesting an area intensively affected by rock solution processes and the development of epikarst, especially within the upper 10 m (30 ft) of rock column (Fig 5). Epikarst is characterized by highly weathered carbonate rock with high porosity and permeability. Additionally, we mapped linear features within the two main waterbodies to be monitored north and south of the plant (Fig 6).


**Figure 1:** Main linear features in the Lower Keys around Cudjoe Key, mostly defined by alignment of shorelines and channels

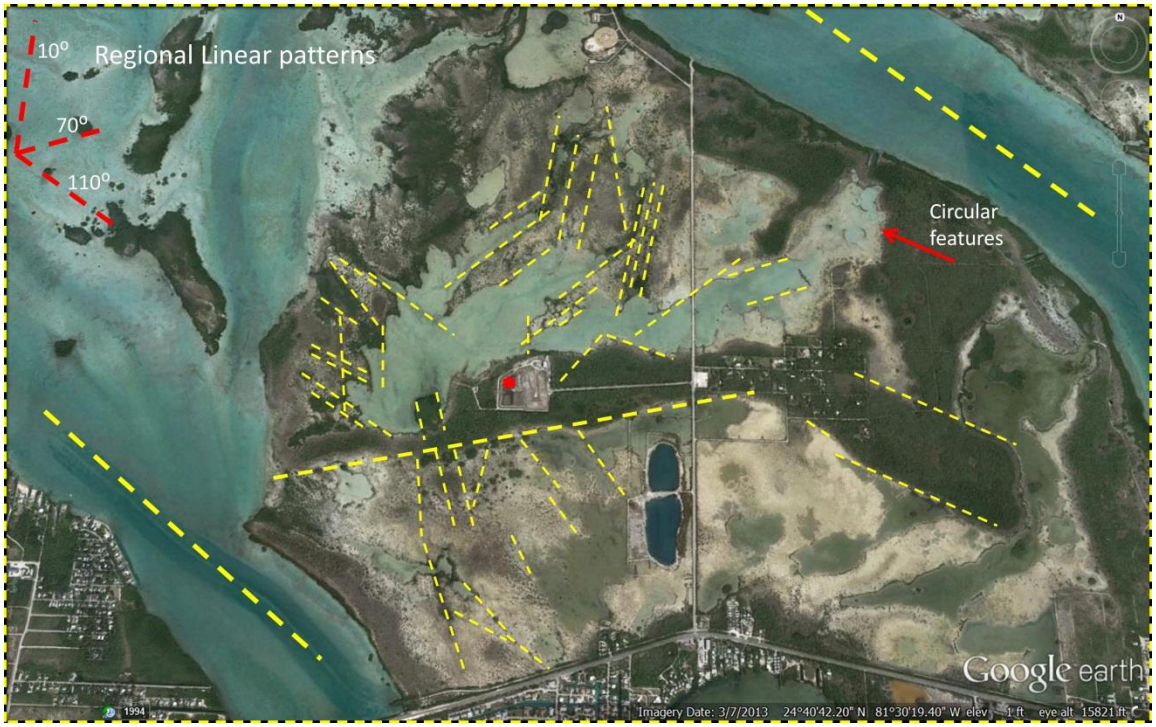


**Figure 2:**. Linear feature map of Cudjoe Key. A significant number of linear features in Cudjoe have similar trend as those identified at regional scale (Lower Keys scale), especially those sets with azimuth 70$^{O}$ and 110$^{O}$ (heavy lines)

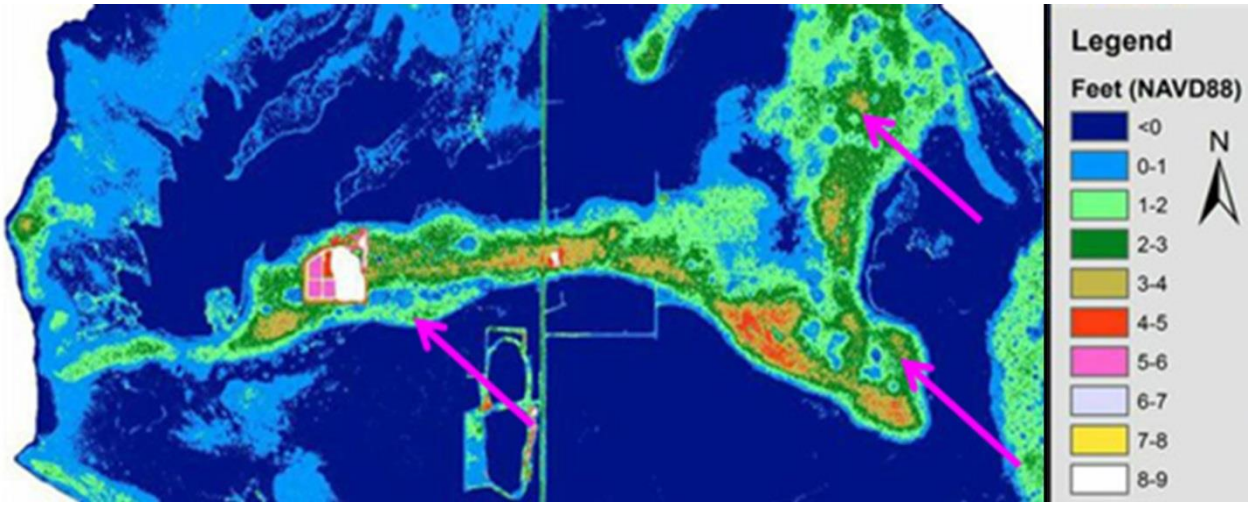


**Figure 3:** Lidar image of central portion of Cudjoe Key. Arrows show areas where circular features are abundant

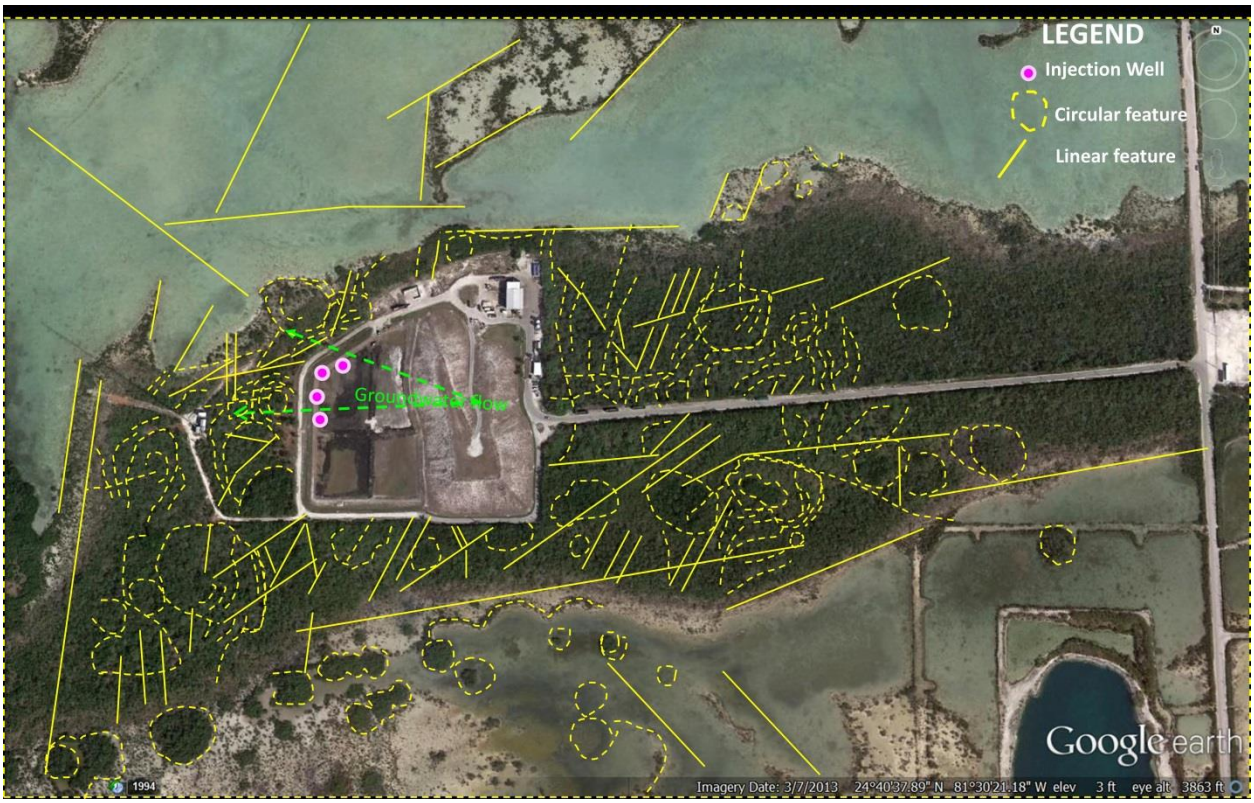


**Figure 4:** Satellite image (Google) with delineation of potential epikarst features. Also shown in green are preferential groundwater flow directions calculated from stage elevation at shallow (20 ft) observation wells (LANGAN 2014)

**Figure 5:** Karst shaft. Typical epikarst feature consisting of a circular vertical shaft resulting from the enlargement of the intersection of two fractures systems. Located 20 ft west of the southernmost concrete anchor of the antenna guys, west of the AWTP


**Figure 6:** Satellite image (Google) with delineation of linear features (in red) within waterbodies selected for monitoring

# Regional Stratigraphy to Local Geology

Besides information from remote sensing techniques (linear and circular feature mapping) we tapped on the available geological information to postulate the stratigraphic relationships in Cudjoe Key. As can be observed in Fig 7, the section at Cudjoe Key should consist of an upper section of close to 30' of oolitic carbonate rocks belonging to the Miami Oolite, underlain by coralline boundstones which change into packstones and wackestones with depth.

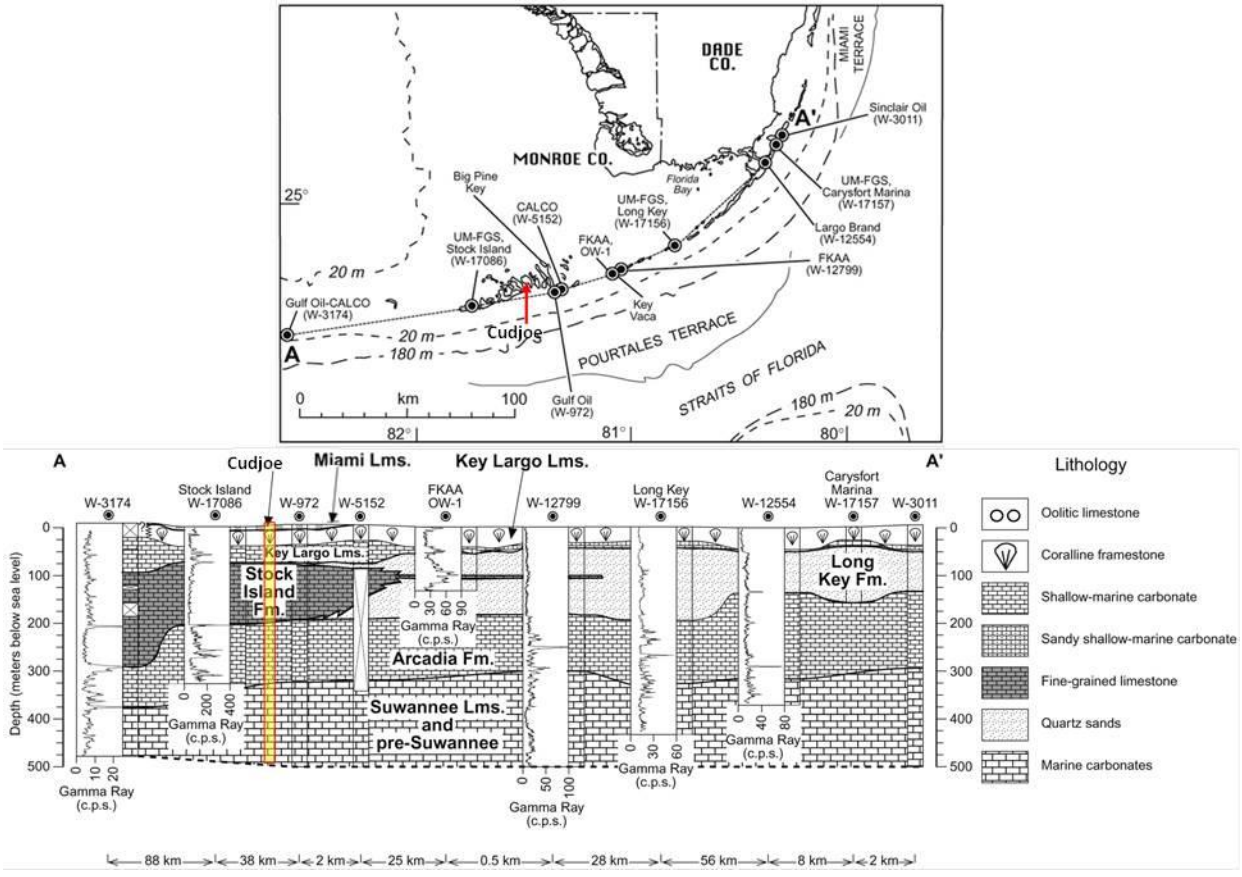


**Figure 7:** Southwest-to-northeast stratigraphic cross section along the Florida Keys from the Dry Tortugas (A) to Key Largo (A'). Also shown is Cudjoe Key (above) and approximate location of stratigraphic column at Cudjoe (yellow column). Modified from Cunningham et al. 1998.

Geological information from records obtained during drilling of observation and injection wells (logging) at Cudjoe Key is meager, mostly because descriptions were not intended for stratigraphic studies. A brief identification of rock types and textures from rock cuttings collected during drilling of injection wells allow the identification of the following: 1) existence of oolitic rocks on surface and extending to 30-32 ft; 2) a discontinuity at about 30-32 ft marked by sandy carbonates underlain by coralline boundstone which in turn extends down to about 42 ft; and 3) a discontinuity at about 100-110 ft where sandy carbonates overlie pervasive solution features on top of wackestones/packstones.

The upper 32' include a couple of feet of overburden and about 30 ft of Miami Oolite, overlying the upper coralline-rock rich units of the Key Largo Limestone. That contact between Miami Oolite and Key largo Limestone would correspond to the so called Q4/Q3 surface of Coniglio et al. (1983a, 1983b), developed during exposure of the Key Largo Limestone before deposition of the Miami Oolite. Elsewhere, the Q4/Q3 is characterized by lower permeability locally developing aquitards, (layer of rock  rock with low hydraulic conductivity).and it is underlain by a zone of intense dissolution of the bedrock and the development of high transmissivity. At a depth of about 42 ft there seems to be another discontinuity. In this case, highly permeable coralline boundstones overlie usually less permeable packstones, wackestones and mudstones of the Key Largo Fm.

In summary, from all discussed above we have developed an underground geology model which we think may approach what exists in Cudjoe Key. In Fig 8 we have brought together the information into a conceptual model of underground geology. We used this model as starting point to help the design of the injection experiment and to interpret the results of the various test.

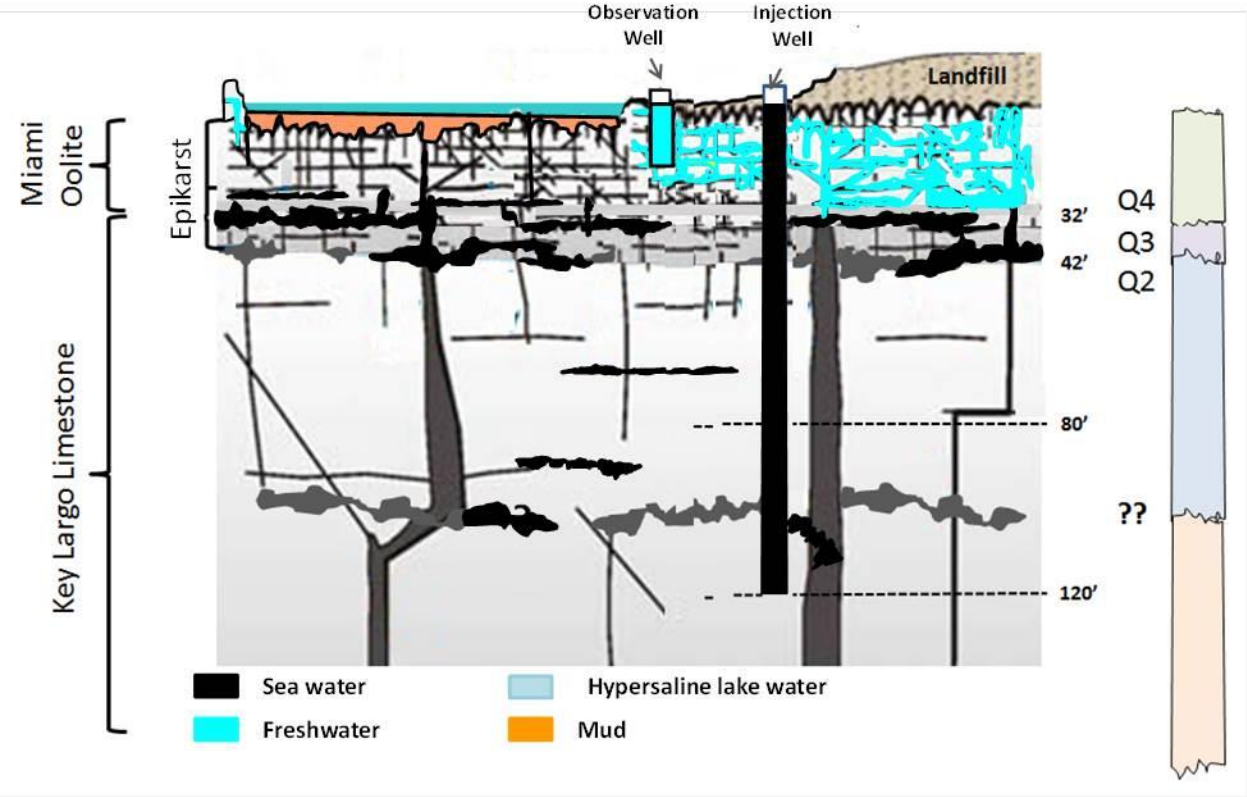


**Figure 8:** Underground Geology Model developed from remote sensing interpretation well-logging information, field work and regional studies.

# Dye-tracer Injection Test Design

Several dye-tracer studies have been performed in the Florida Keys in the past (Paul et al. 1995, 1997; Shinn et al. 1999a, 1999b; Böhlke et al. 1999; and Reich et al. 2001). In most instances the experimental design responded more to the performer's experience than prior assessment of the basic hydraulic and geometric parameters of the rock pile and the appropriate calculation of tracer mass to release. There are at least 33 mass-estimation equations cited in the literature (USEPA 2003) which give as many disparate results for determining the necessary tracer mass, the initial sample-collection time, and the subsequent sample-collection frequency for a proposed tracer test. After comparing all these methodological attempts, a set of new Efficient Hydrologic Tracer-test Design (EHTD) methodology has been developed that combines basic measured field parameters (e.g., discharge, distance, cross-sectional area) in functional relationships that describe solute-transport processes related to flow velocity and time of travel (EPA 2003)

# Efficient Hydrologic Tracer-Test Design (EHTD) Program

The Environmental Protection Agency (EPA) developed the Efficient Hydrologic Tracer Test Design (EHTD) computer program that can be used to estimate tracer mass and transport in tracer experiments. The program integrates measured or estimated field parameters such as discharge, distance, cross-sectional area with functional relationships that describe solute-transport processes related to flow velocity and time of travel (EPA 2003). Hydrological tracer testing is

the most reliable diagnostic technique available for establishing flow trajectories and hydrologic connections and for determining basic hydraulic and geometric parameters necessary for establishing operative solute-transport processes (EPA 2003).

As an analog for the hydrologic system, EHTD assumes a hypothetical continuously stirred tank reactor to develop estimates for tracer concentration and axial dispersion, based on a preset average tracer concentration. Solving the one-dimensional advection-dispersion equation (ADE) provides a theoretical basis for an estimate of necessary tracer mass and sampling frequencies. EHTD simulations have been compared with published tracer-mass estimation equations and suggested sampling frequencies, as well as field measurements obtained from actual tracer tests covering a wide range of hydrologic conditions that included porous-media and karst systems.

We selected EHTD as our basic tool for test design given that comparisons of the actual tracer tests and the predicted results demonstrate that EHTD can reasonably predict that tracer breakthrough, hydraulic characteristics, and sample-collection frequency may be forecasted sufficiently well in most instances to facilitate good tracer-test design (EPA 2003).

A number of test runs were designed to cover the range of operations and hydrological conditions that would characterize the tracer tests in CUDJOE. Some of the parameters required by the EHTD computer program were considered constant for all runs while other where changed for each run. Table 1 shows the basic parameters required by EHTD. Based on reasonable estimates of the EHTD required parameters, we proposed the runs summarized in

Table . The table also shows the resulting tracer mass estimate in each case.

**Table 1:** Dye Dispersion Scenarios

| Parameter | Description |
|---|---|
| Distance | Distance from injection point to measurement point |
| Thickness | Injection well effective open length |
| Injection discharge | Discharge at injection well |
| Discharge at obs. Point | Approximate discharge at measurement point |
| Release time | Tracer release time |
| Porosity | Aquifer porosity |

**Table 2:** EHTD Run for CUDJOE Tracer Test Design.

| Run | Distance from injection point to measurement point | Thickness | Injection discharge | Discharge at obs. Point | Release time | Porosity | Estimated dye mass | Estimated dye mass |
|---|---|---|---|---|---|---|---|---|
| | m | m | m3/h | m3/h | h | | g | kg |
| 1 | 90 | 10 | 74.9 | 3.60E-01 | 1 | 0.34 | 3.95E+03 | 3.95 |
| 2 | 90 | 20 | 74.9 | 3.60E-01 | 1 | 0.34 | 7.91E+03 | 7.91 |
| 3 | 90 | 30 | 74.9 | 3.60E-01 | 1 | 0.34 | 1.19E+04 | 11.86 |
| 4 | 200 | 10 | 74.9 | 3.60E-01 | 1 | 0.34 | 8.78E+03 | 8.78 |
| 5 | 200 | 20 | 74.9 | 3.60E-01 | 1 | 0.34 | 1.76E+04 | 17.57 |
| 6 | 200 | 30 | 74.9 | 3.60E-01 | 1 | 0.34 | 2.63E+04 | 26.35 |
| 7 | 90 | 10 | 74.9 | 3.60E-01 | 8 | 0.34 | 3.95E+03 | 3.95 |
| 8 | 90 | 10 | 74.9 | 3.60E-01 | 8 | 0.60 | 6.97E+03 | 6.97 |
| 9 | 200 | 10 | 74.9 | 3.60E-01 | 1 | 0.60 | 1.55E+04 | 15.50 |
| 10 | 500 | 10 | 74.9 | 3.60E-01 | 1 | 0.34 | 2.20E+04 | 22.00 |
| 11 | 90 | 10 | 74.9 | 3.60E+01 | 1 | 0.34 | 597.00 | 0.60 |
| 12 | 200 | 10 | 74.9 | 3.60E+01 | 1 | 0.34 | 131.00 | 0.13 |
| 13 | 500 | 10 | 74.9 | 3.60E+01 | 1 | 0.34 | 324.00 | 0.32 |

The maximum tracer mass of 26.35 kg corresponds to the scenario when the well effective length is assumed to be 30 m and discharge at the measurement point is considered very small. This corresponds to relatively low permeability case with low crack density in the aquifer. Other runs represent situations where the permeability is higher and consequently discharge at the measurement point is assumed much higher.

Figure 9 presents the estimated evolution of the tracer concentration at a measurement point located 90 m away from the injection well and parameters corresponding to Run 11. For this case, the detection threshold assumed to be 5 µg/L occurs around the hour 105 approximately after the tracer injection has occurred. The concentration peak happens at 156 hours after the injection.

Figure 10 shows the estimated evolution of the tracer concentration at 200 m from the injection well corresponding to Run 12. In this case, the detection threshold of 5 µg/L is first passed at hour 230 approximately after the tracer injection has occurred. The concentration peak occurs at 336 hours after the injection.

Figure 11 depicts the estimated evolution of the tracer concentration at a measurement point located 500 m away from the injection well. For this case, the detection threshold is surpassed 620 hours approximately after the tracer injection. The concentration peak happens 902 hours after the injection.

In conclusion, the application of the EPA Efficient Hydrologic Tracer Test Design (EHTD) computer program to support the injection well tracer test design at Cudjoe Key, allowed to estimate the tracer mass and sampling frequency. The results of the EHTD application recommended a tracer mass of 30 kg which should allow measurement above the assumed concentration threshold of 5 µg/L starting at 4, 10 and

26 days after dye injection at measurement distances of 90 m, 200 m and 500 m respectively. We must keep in mind that EHTD is primarily intended as a support program to obtain reasonable estimates of tracer mass and sampling rates.

Finally, it is important to keep in mind that EHTD does not provide a full representation of the aquifer and consequently its application to the CUDJOE site does not reflect exactly the hydrologic and solute transport response of the aquifer. Since several of the program assumptions may not be completely adequate for this site, results should be considered a first approximation to support the tracer test design. Real sampling times may differ from those estimates shown in the runs presented in this document.

We selected Sodium Fluorescein (also called Uranine) and Rhodamine WT (Rhodamine) for carrying out the test, given these are environmentally friendly dyes approved by the EPA, with moderate to very low sorption tendency (conservative tendency), strong spectral intensity, well developed analytical techniques, very distinctive color contrast, and relatively low cost of analysis. Fluorescein has only one handicap, it tends to photodecay. Although it is not a problem for groundwater sampling, surface measurements and sampling need to take this into consideration because sunlight may diminish total mass recovery. To be on the safe side and considering the possibility of finding higher porosity (>34%) we injected 30 Kg of Fluorescein dissolved in 60 gallons of tap water, the same water was going to be used as chaser and continuous injection following the dye.

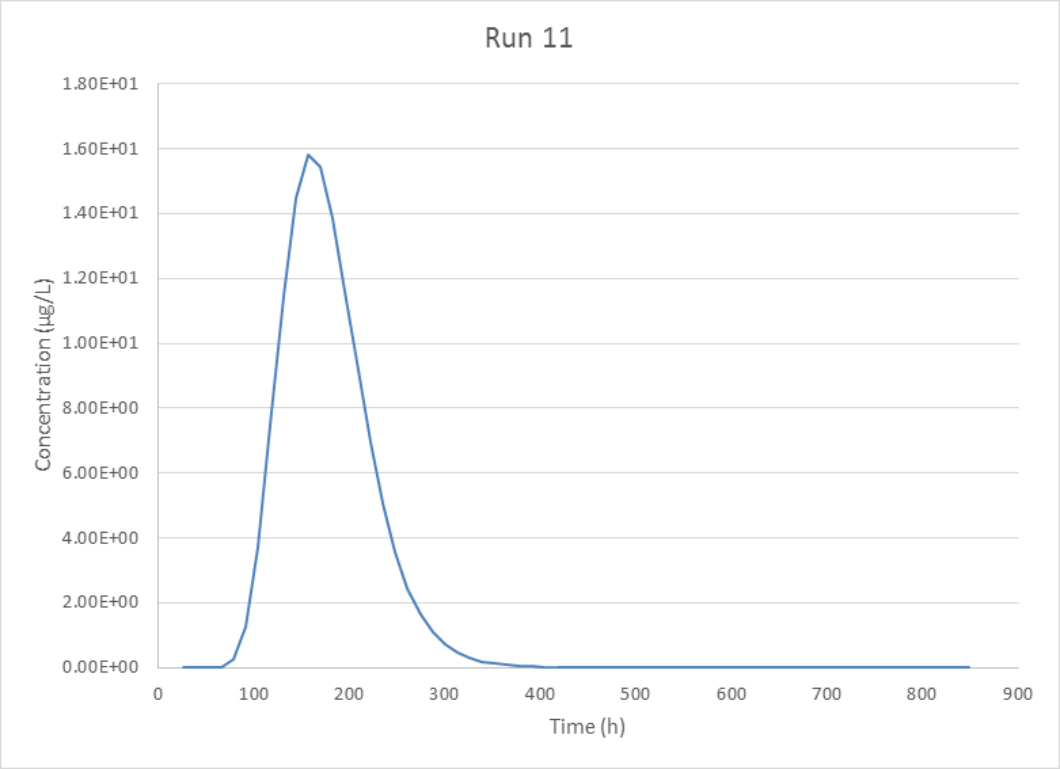


**Figure 9:** Calculated concentrations vs time at a measurement point located at 90 m

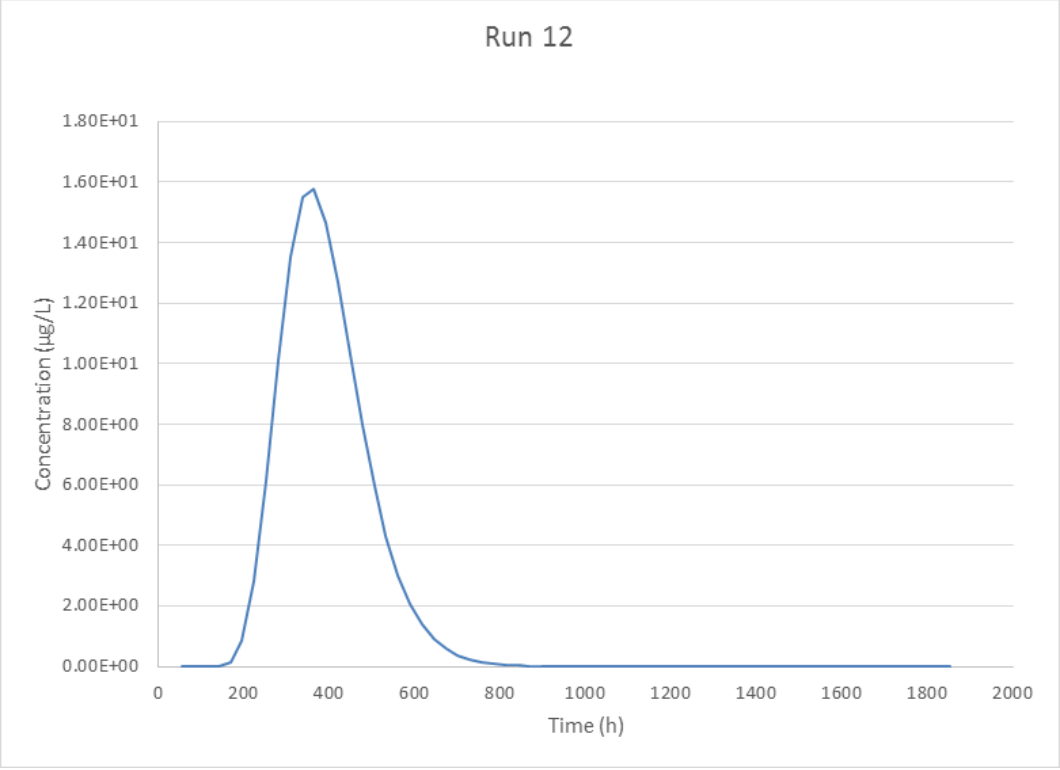


**Figure 10:** Calculated concentrations vs time at a measurement point located at 200 m

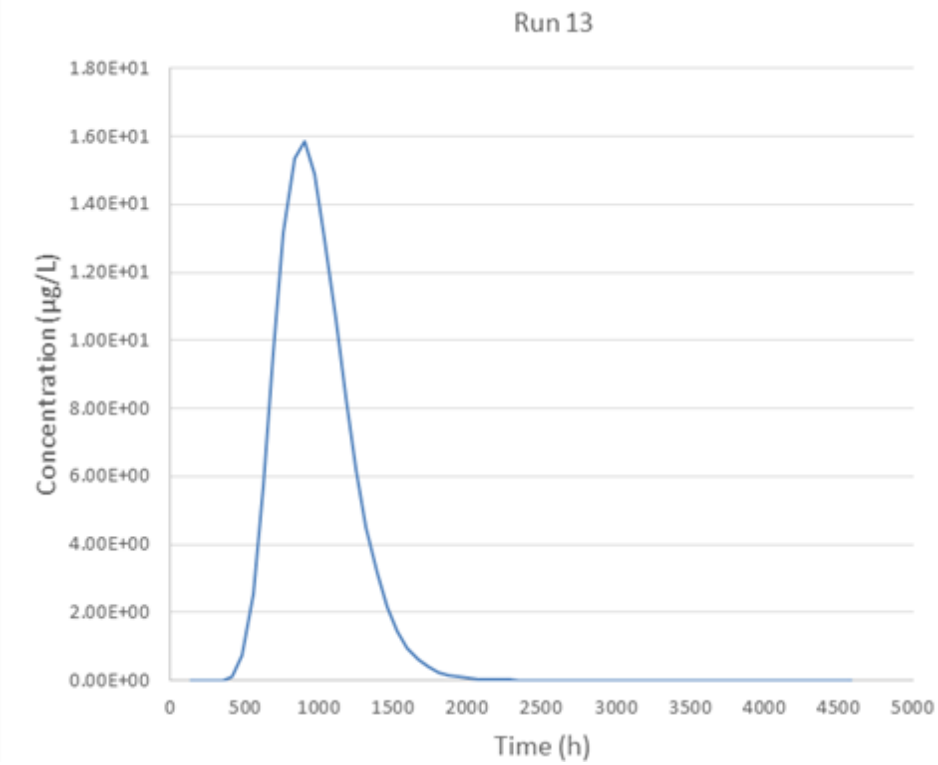


**Figure 11:** Calculated concentrations vs time at a measurement point located at 500 m

# Baseline Study .

We subdivided the study into four main phases, Modeling, Baseline characterization, Freshwater Injection test and dye-tracer Injection test. In order to establish a Baseline we characterized the ground and surface waters at Cudjoe Key, in such a way that we could directly assess those changes induced by the different test by comparing with the Baseline. In this context the Baseline assessment corresponds to the "Before" phase of a Before-and-After experiment.

The following tasks are intended to establish current conditions regarding Fluorescein and/or Rhodamine concentrations in surface and underground waters of Cudjoe Key, around and under the Advanced Treatment Wastewater Facility (AWTF).Baseline determination was planned for 2 or 3 days, but lasted eight days due to unintended delays from 2/17/2015 to 2/25/2015. The following activities were completed to define a baseline and characterize the system:

1- Wells were purged 1½ well volumes and left to recover for 24 hours before sample collection began. For the water sampling from wells we used ISCO Autosamplers programmed to collect water samples pumped periodically from a depth of 100 ft for injection wells (IWs). Likewise, water samples were pumped periodically from depths ranging from 4 to 15 ft below ground surface for observation wells (OWs). Samples collected from the wells were placed in dark amber polypropylene bottles and analyzed at installed lab on site.

2- ISCO Autosamplers were connected to ¾" polypropilene tubing and introduced into the wells and (Fig 12). pumped

water directly from the wells every hour. Sample volume varied from 200 to 800 ml. A total of six autosamplers were permanently deployed.

3- Baseline assessment of water physicochemical properties in lake waters located North of AWTF, as well as the ponds located immediately to the South of AWTF. The assessment was done with continuous recording of physicochemical properties and dye concentrations along transects (Fig 13 and 14). Technological advances in the last decade allow the determination of dye-tracer in water at extremely low concentration (parts per trillion). We used three types of fluorometers to measure dye-concentration in waters, a field deployable Turner C3® Submersible Fluorometer, an Aqualog® Benchtop Horiba Spectrofluorometer and a Shimadzu Model RF-m-150 Fluorometer installed on site, in a trailer at Cudjoe Key.

4- The C3® field fluorometer was deployed on a floating platform (Fig 13 and Table 3) together with a YSI sonde, and a GPS. From this platform we measured dye and physicochemical variables along transects in water bodies to the North and South of the AWTF. The multi-sensor, water quality monitoring instrument (YSI Model 6600 V2 sonde) measured salinity (PSU), specific conductance (µS $cm^{-1}$), temperature (°C), dissolved oxygen (DO; mg $l^{-1}$), %DO Saturation and pH. Additionally, for sake of quality control procedures water samples were also collected randomly along transects to be later analyzed by the spectrofluorometer.

5- Instruments were deployed on an unmanned surface vessel (USV) to transit approximately 4-6 miles of transects (Fig 15). We deployed a TURNER C3 submersible fluorometer to measure dye concentration and a multi-sensor, water quality monitoring instrument (YSI sonde) to measure Temperature, Dissolved Oxygen, pH, Salinity (plus Specific Conductance). The USV (Fig 13) was developed

to support autonomous survey missions in shallow and coastal marine habitats. The USV can operate in waters as shallow as ~0.5 m.

*6-* The pond south of the AWTF resulted too shallow and too seagrass laden for the USV that we had to resort to kayaks to maneuver its waters. For the lake north of the AWTF, the combination of shallow waters, winds and tides prevented the use of the USV in several instances. We used a Jonboat instead.

7- Fluorescein has been used to color automobile antifreeze for many years as well as Rhodamine. These dyes were present in small quantities in shallow ground waters, suggesting they came from the sanitary fill at Cudjoe Key. Additionally several organic compounds may interfere with the spectral response of dyes. To avoid signal interference with those of Fluorescein and Rhodamine and designed analytical methods to isolate our injected dye signal (See Appendix 1).

8- Background concentrations of both Fluorescein and Rhodamine were determined at each selected well during the first three sampling surveys, CK01 to CK03. A summary of results is shown in Table 4.


**Figure 12:** Connecting ISCO Autosampler to OW2


**Figure 13:** Unmanned surface vessel (USV) in Cudjoe Key deploying a submersiblefluorometer to measure dye concentration, and a multi-sensor, water quality monitoring instrument (YSI sonde) to simultaneously measure physiochemical parameters of water quality.

**Table 3:** Technical specifications for TURNER C3® Submersible Fluorometer (ppb= parts per billion)

| | Detection Limit | ConcentrationRange |
|---|---|---|
| Fluorescein Dye | 0.01 ppb | 0-500 ppb |
| Rhodamine Dye | 0.01 ppb | 0-1000 ppb |


**Figure 14:** Designed transects for dye and physical-chemical WQ determinations

**Table 4:** Baseline average concentration of Fluorescein and Rhodamine

| Collection site | Samples collected | Average concentration of fluorescein (ppb) | Average concentration of rhodamine (ppb) |
|---|---|---|---|
| OW1 | CK01- 2/21/15-2/22/15 (24 samples) | 0.448 ± 0.0164 | 0.131 ± 0.0364 |
| | CK02- 2/22/15-2/24/15 (24 samples) | | |
| | CK03- 3/3/15 (14 samples) | | |
| OW2 | CK01- 2/20/15-2/21/15 (24 samples) | 0.105 ± 0.0094 | 0.0331 ± 0.00287 |
| | CK02- 2/22/15-2/24/15 (23 samples) | | |
| | CK03- 3/3/15 (15 samples) | | |
| OW4 | CK01- 2/20/15-2/21/15 (24 samples) | 0.495 ± 0.0516 | 0.123 ± 0.044 |
| | CK02- 2/21/15-2/23/15 (24 samples) | | |
| | CK03- 3/3/15 (15 samples) | | |
| OW5 | CK01- 2/20/15-2/21/15 (24 samples) | 1.198 ± 0.124 | 0.331 ± 0.060 |
| | CK02- 2/21/15-2/23/15 (24 samples) | | |
| | CK03- 2/24/15, 3/3/15 (15 samples) | | |
| IW1 | CK01- 2/21/15-2/22/15 (24 samples) | 0.790 ± 0.00958 | 0.0306 ± 0.0307 |
| | CK02- 2/22/15-2/24/15 (24 samples) | | |
| | CK03- 3/3/15 (14 samples) | | |
| IW4 | CK01-2/22/15 (2 samples) | 0.0694 ± 0.0272 | 0.0415 ± 0.0325 |
| | CK02- 2/22/15-2/25/15 (17 samples) | | |
| | CK03- 3/3/15 (14 samples) | | |

# Freshwater Injection

Freshwater injection was proposed as a pre-dye injection stage with two main objectives, to prepare the ground to conditions approaching future operating conditions of the AWTF plant while injecting the dye, and to test for connectivity of the aquifers by monitoring salinity changes, an objective partially hampered by extensive flooding of the injection wells area during the first freshwater injection attempt. The target was to inject close to 1 million gallons in a two-day injection. After resuming freshwater injection, intensive bubbling began to occur in the nearby puddle (Fig 15) which later became active venting from the bottom of the puddle with muddy water rising from openings in that bottom (Fig 16). This intensive venting lasted until soon after the end of freshwater injection. This injection phase was concluded on March 4rd, after injecting about 1.86 million gallons of freshwater.

**Figure 15:** Extensive bubbling in puddle near injection well

**Figure 16:** Muddy freshwater springs venting at the puddle bottom by IW3

We interpreted the bubbling as ascending air bubbles due to pore space filling and soil/bedrock saturation by both, freshwater sinking from the puddle, and mostly by injected freshwater rising due to buoyancy on top of saline waters of the deeper aquifer. It was more evident yet when turbid waters from below were coming to the puddle as springs, even when tidal cycle was receding, lowering sea level. We must then reassess the previous ground geology model of Figure 8 to incorporate these connections from injection level (80-120 ft) and surface waters as shown in Figure 17. These connections would function as conduits to rising freshwater (Fig 18).

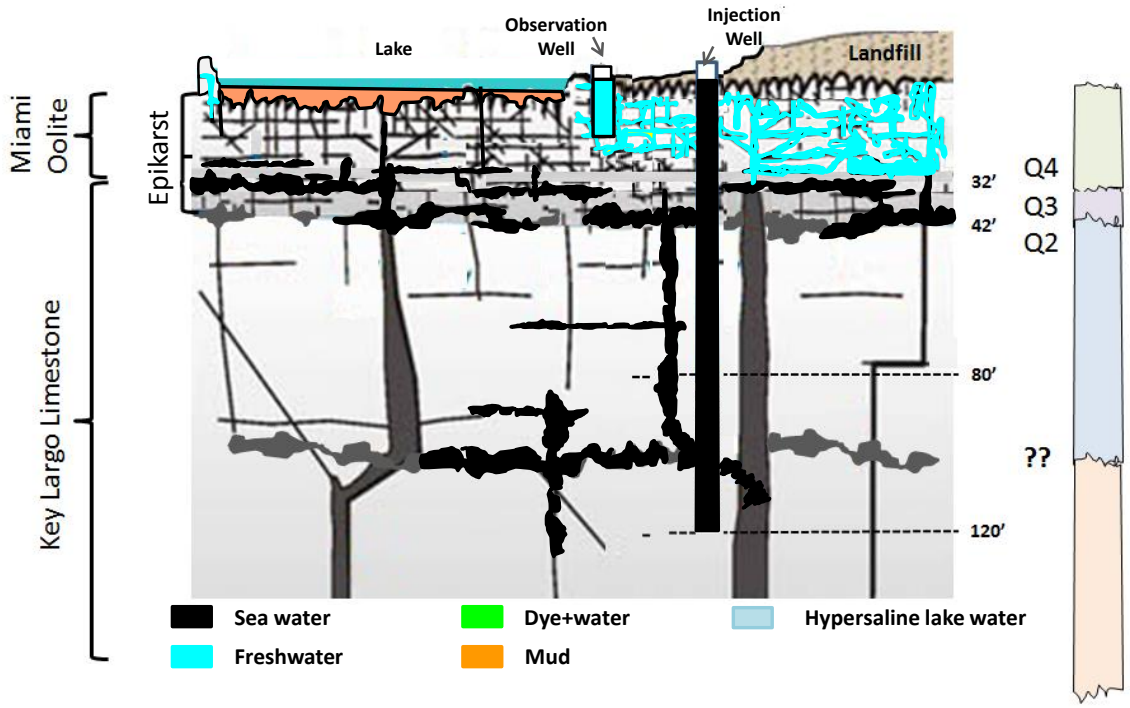


**Figure 17:** Reassessed underground geology for Cudjoe Key site

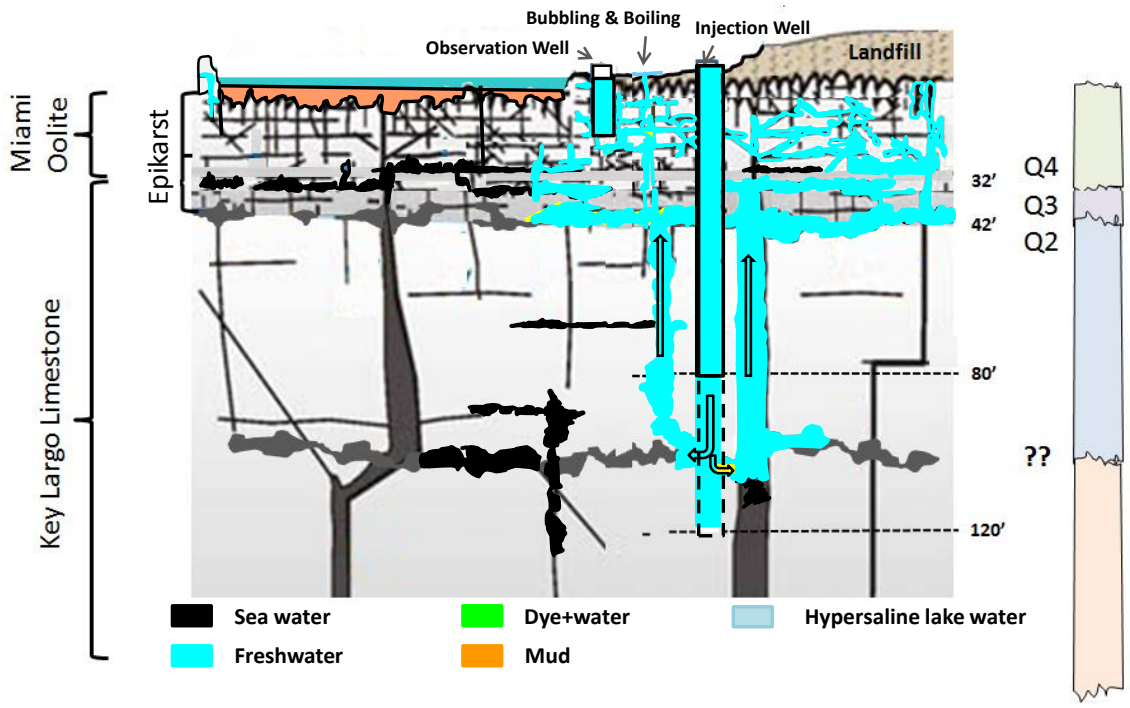


**Figure 18:** Conceptual rendition of interpreted interconnected underground network during freshwater injection

# Dye-tracer Injection

Dye-tracer injection was performed on March 5th, at 8:00 AM. Thirty kilograms of Fluorescein were diluted in tap water to make 60 gallons of solution which were poured directly into IW3. Freshwater injection was resumed at an average rate of 424 gal/min or approximately 610,600 gal/day. Monitoring was continued at IW1 and IW4, as well as OW1, OW2, OW4 and OW5. Daily transects were measured on the northern lake and southern pond using the Turner C3 Submersible fluorometer and a YSI sonde. Additionally, given the low concentrations observed in the water bodies during Baseline and Freshwater Injection stages, water samples were collected randomly along transects to verify Uranine content with the highly sensitive Horiba Spectrofluorometer.

After partial results and findings were presented to the FKAA on March 19th, indicating the high probability of existence of an underground connection between the injection depth and the unconfined aquifer, the FKAA decided to cease all sampling operations and injection on March 26th, 2015. We retrieve the already collected samples until March 26th and analyzed them for Fluorescein content.

# Results of dye-tracer Injection

We present the final results in Figures 19 to 25 to illustrate and track the changes observed at each monitoring site and transects using box-plot diagrams (left panel) and time series of Uranine (right panel) at each monitoring locality. The upper and lower borders of the box are the 75th and 25th percentiles respectively, while the upper and

lower whiskers indicate the 95$^{th}$ and 5$^{th}$ percentiles respectively. The horizontal line inside the box corresponds to the median value. Finally, isolated values above the upper or below the lower whiskers are anomalous concentrations.

Time-series plots (right panel) show the linear trend (black line) and its least-square fit equation, as well as the 95$^{th}$ percentile concentration (dashed blue line) and the dye injection date (red line). Values above the dashed blue line are considered anomalous. Figures 19 and 20, for IW1 and IW4 respectively, illustrate the dynamics of dye circulation at injection depths, while those of Figures 21 to 25 show the dynamics of shallow depth and surface dye behavior.

Figure 19 shows Injection well 1 (IW1) slightly increasing Uranine concentration from Baseline (BSL) into Freshwater Injection stage (FWI) and further significant increases after dye-tracer injection (INJ). Details on the right panel highlight the rapid appearance of the first arrival (FA) as a significant anomaly six hours after dye injection, followed by several anomalies 12 days later. The occurrence of anomalies in IW1 were expected given its closeness to the dye injection well (IW3), but such a small increase was not. It is perhaps indicative of a rapid upward movement of the fresh water-dye mix.

Injection well 4 (IW4) displays little change in the mean from BSL to INJ, but a clear pattern change following dye-injection. A relatively high value appeared during BSL, illustrating the already variable setting. What we consider highly anomalous values arrived 37 hours after injection. Again, although anomalous, concentrations are very low.

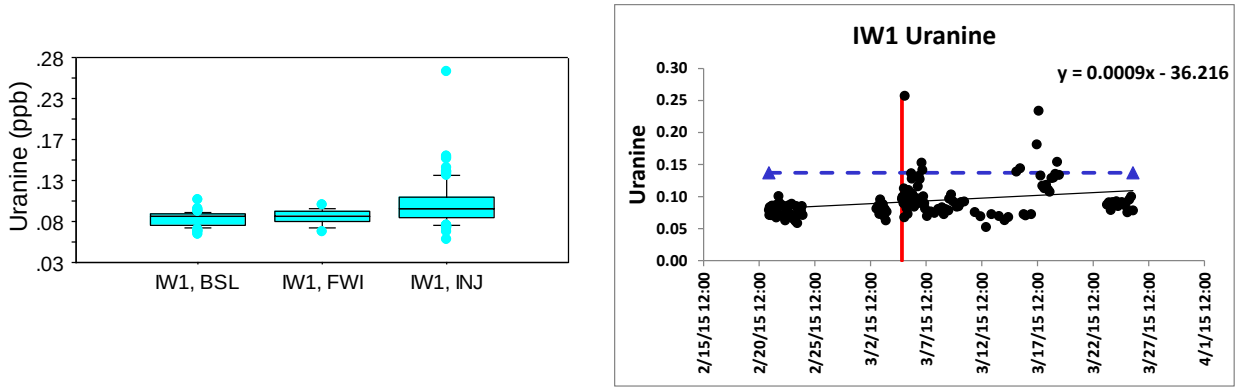


**Figure 19:** The left panel is a box plot diagram of Uranine concentrations observed at **Injection Well 1** during Baseline (BSL), Freshwater Injection (FWI) and Dye-tracer Injection (INJ) stages. The right panel shows the same data but as a time-series

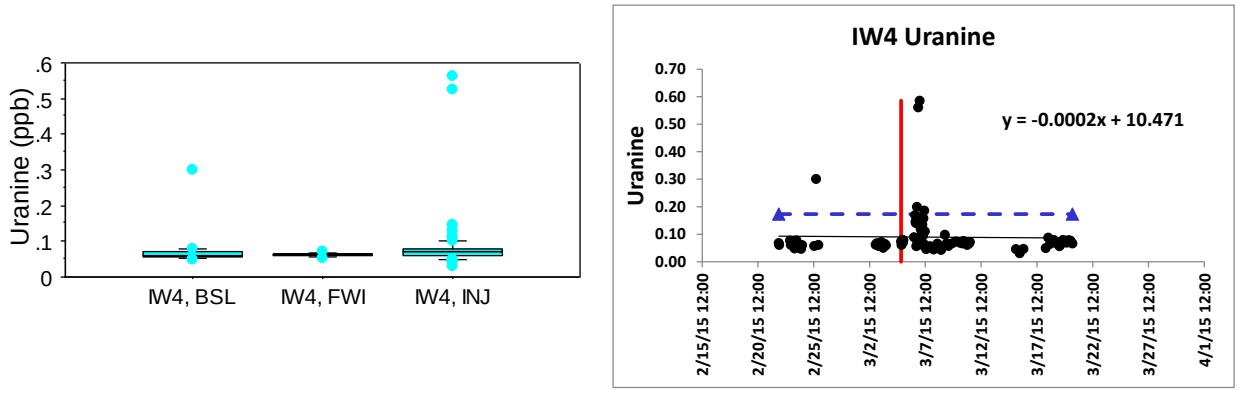


**Figure 20:** The left panel is a box plot diagram of Uranine concentrations observed at **Injection Well 4** during Baseline (BSL), Freshwater Injection (FWI) and Dye-tracer Injection (INJ) stages. The right panel shows the same data but as a time-series.

As shown in Figure 21, OW1 displays the highest Uranine concentrations in the baseline period, followed by a decline to FWI and even further decrease during INJ phase It is apparently caused by dilution by tap-water injection. Despite overall lower values during INJ, the occurrence of a barely anomalous concentration 10 hours after dye

injection suggest this as first arrival (FA) of Uranine to OW1, hence, an estimated flow velocity of 23 m/h from injection well (IW3) to OW1.

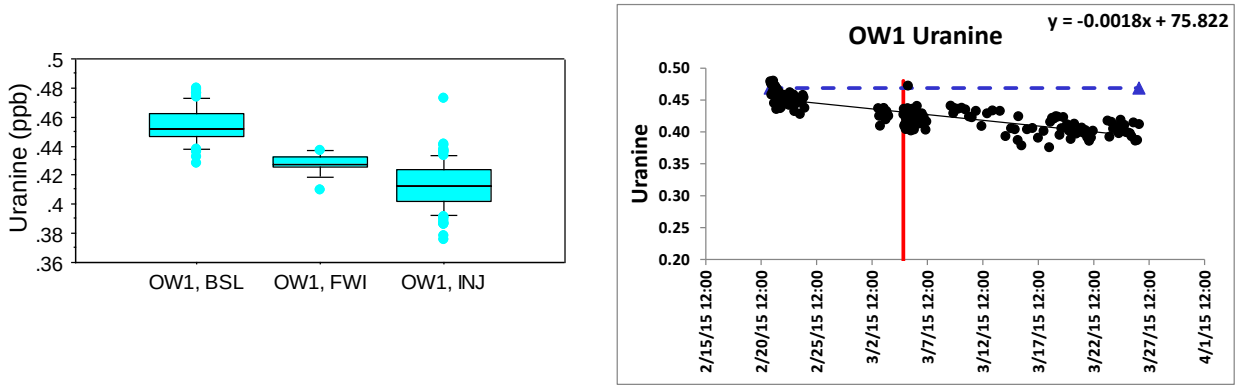


**Figure 21:** The left panel is a box plot diagram of Uranine concentrations observed at **Observation Well 1** during Baseline (BSL), Freshwater Injection (FWI) and Dye-tracer Injection (INJ) stages. The right panel shows the same data but as a time-series.

OW2 displays just a slight increase from BSL to FWI but overall constancy in the mean. What is important is the significant occurrence of high anomalous values after dye-injection. First arrival took place 16 hours after injection, indicating a velocity of groundwater flow of 14 m/h.

OW4 shows a statistically significant drop in Uranine concentration from BSL to FWI and into INJ. Despite this decline, there are two departures after injection, one of them statistically significant (>95$^{th}$ pctl). If that value represented a FA occurring at about 17 hours after injection, then the corresponding flow velocity would be of about 9 m/h.

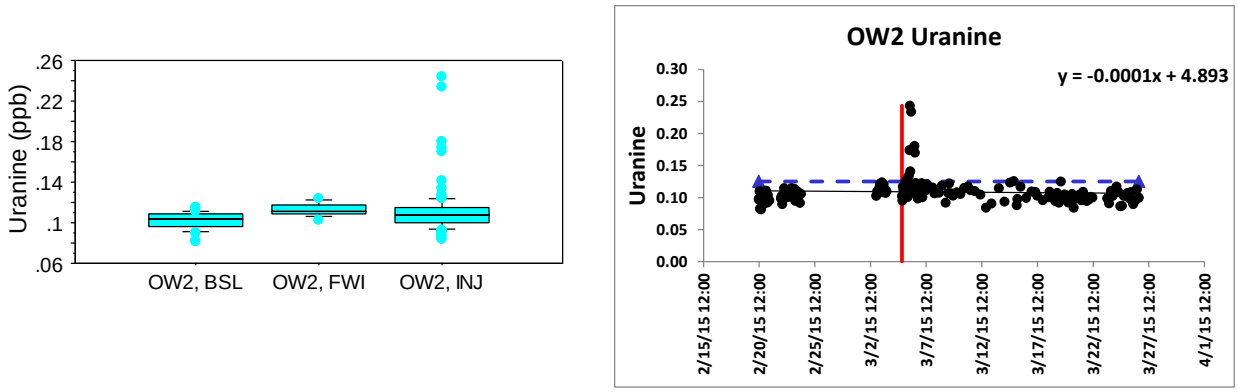


**Figure 22:** The left panel is a box plot diagram of Uranine concentrations observed at **Observation Well 2** during Baseline (BSL), Freshwater Injection (FWI) and Dye-tracer Injection (INJ) stages. The right panel shows the same data but as a time-series.

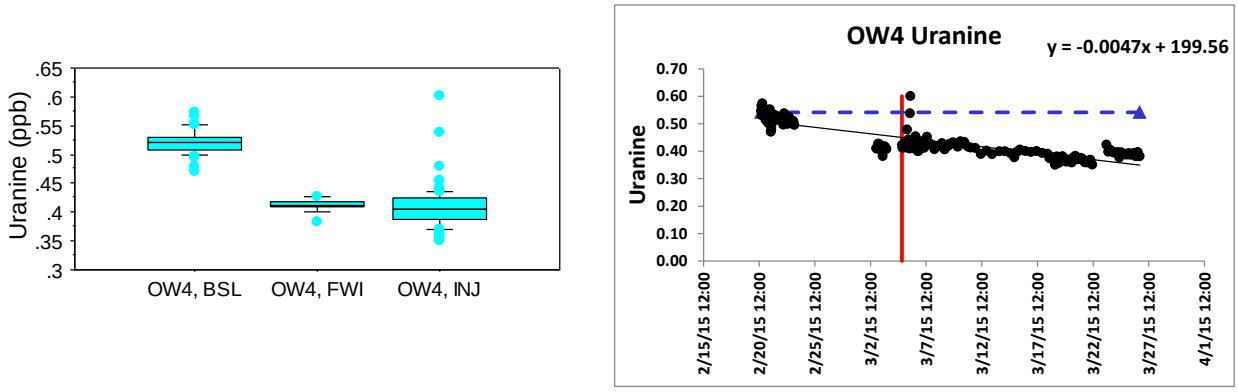


**Figure 23:** The left panel is a box plot diagram of Uranine concentrations observed at **Observation Well 4** during Baseline (BSL), Freshwater Injection (FWI) and Dye-tracer Injection (INJ) stages. The right panel shows the same data but as a time-series.

Finally, OW5 also shows a marked drop in Uranine concentration with tap water injection which continues four days after dye injection, when a slightly increasing tendency began. By the end of the period of record, eighteen days after injection, concentrations were back to BSL levels. Results from this well, located very close to the injection well site, clearly illustrates the effect of tap water flooding.

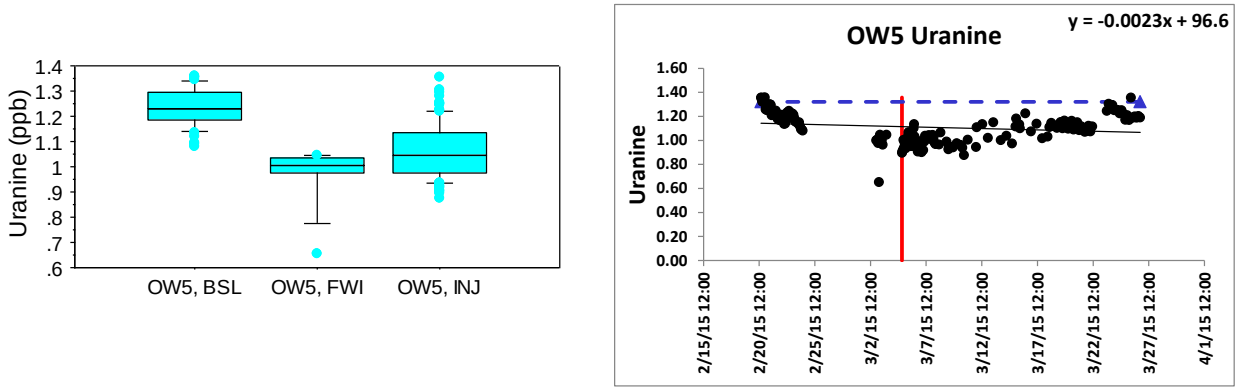


**Figure 24:** The left panel is a box plot diagram of Uranine concentrations observed at **Observation Well 5** during Baseline (BSL), Freshwater Injection (FWI) and Dye-tracer Injection (INJ) stages. The right panel shows the same data but as a time-series.

Measurements along transects using the C3 submersible fluorometer were performed before and after dye injection in the Northern Lake. Given that the southern pond is within land owned by the US Fish and Wildlife Service, transects in the pond were only measured after the USFWS granted access to their land, and when dye-injection had already begun. The exception was a sample collected from the pond during inspection of the study area on February 17$^{th,}$, 2015.

Spectrofluorometer analysis of Uranine in water samples from the northern lake and the southern pond were only performed after dye-injection, as shown in Figure 25. The lake rendered two anomalies up to 8 times average concentration level, occurring 13 days after dye-injection, and superimposed on a rather low-concentration and constant trend. These anomalies occurred close to the north shore of the lake where a series of linear features seem to converge (Fig 6). The South Pond increased dye-concentrations continuously after injection and shows values reaching anomalous concentration 18 and 19 days after injection.

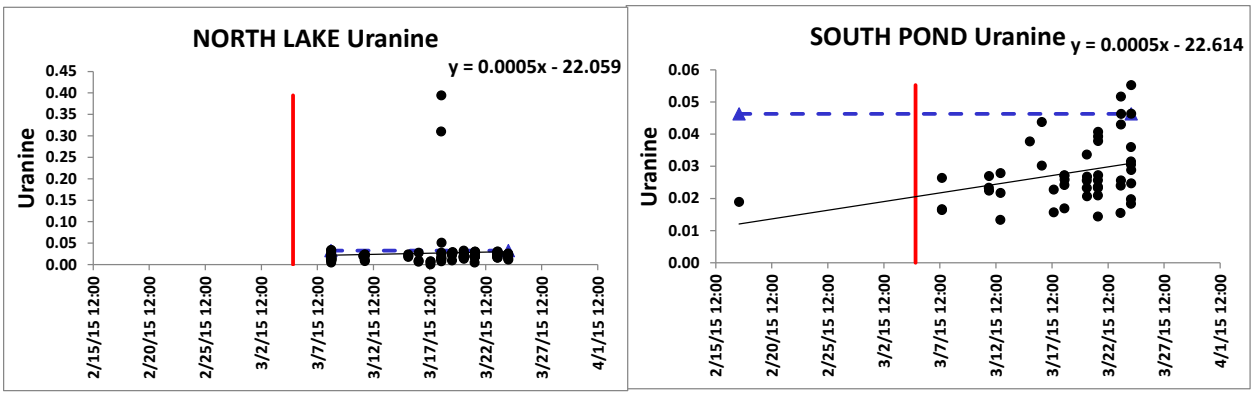


**Figure 25:** Time-series of Uranine concentrations observed in water samples collected in the Northern Lake and Southern Pond after dye-tracer Injection (INJ) stage.

Arrival times and distance from injection well were used to estimate underground flow velocity as shown in Table 5 and Figure 26. With those results we constructed the diagram of Figure 27, where a hypothetic flow velocity field for injection to surface sites has been constructed. An important observation is that the azimuth of the highest velocity vector coincide very closely with one of the regional linear feature trends (70$^{O}$), thought to represent large and deep seated fracture systems in the Lower Keys and Cudjoe Key (Figure 1 and 2).

**Table 5:** Calculation of groundwater flow velocities from Fluorescein arrival times

| | Arrival time (h) | distance (ft) | flow velocity (ft/h) |
|---|---|---|---|
| **IW1** | 5.92 | 66 | 11 |
| **IW4** | 47.12 | 164 | 3 |
| **OW1** | 10 | 758 | 76 |
| **OW2** | 16 | 745 | 47 |
| **OW4** | 16.92 | 509 | 30 |
| **To Lake** | 317 | 2680 | 8 |

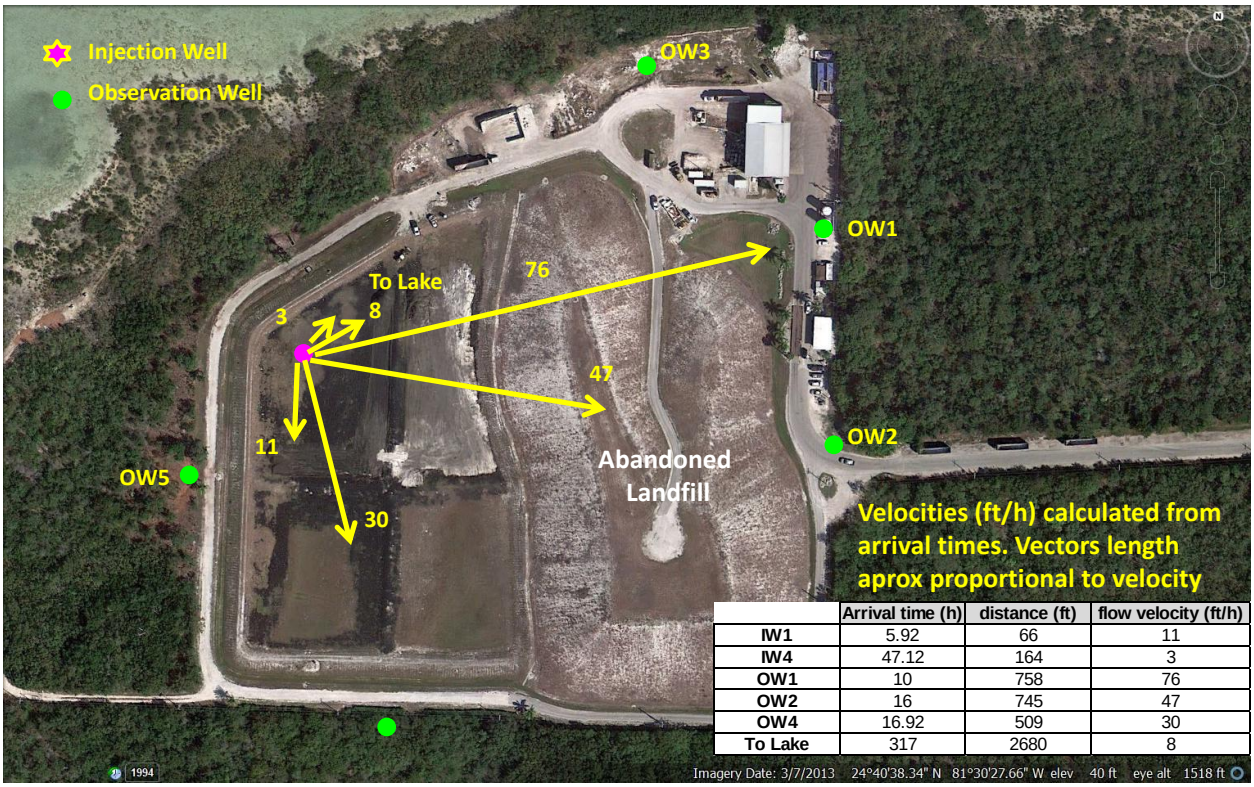


| | Arrival time (h) | distance (ft) | flow velocity (ft/h) |
|---|---|---|---|
| IW1 | 5.92 | 66 | 11 |
| IW4 | 47.12 | 164 | 3 |
| OW1 | 10 | 758 | 76 |
| OW2 | 16 | 745 | 47 |
| OW4 | 16.92 | 509 | 30 |
| To Lake | 317 | 2680 | 8 |

**Figure 26:** Flow velocity vectors showing relative flow velocities in Cudjoe Key

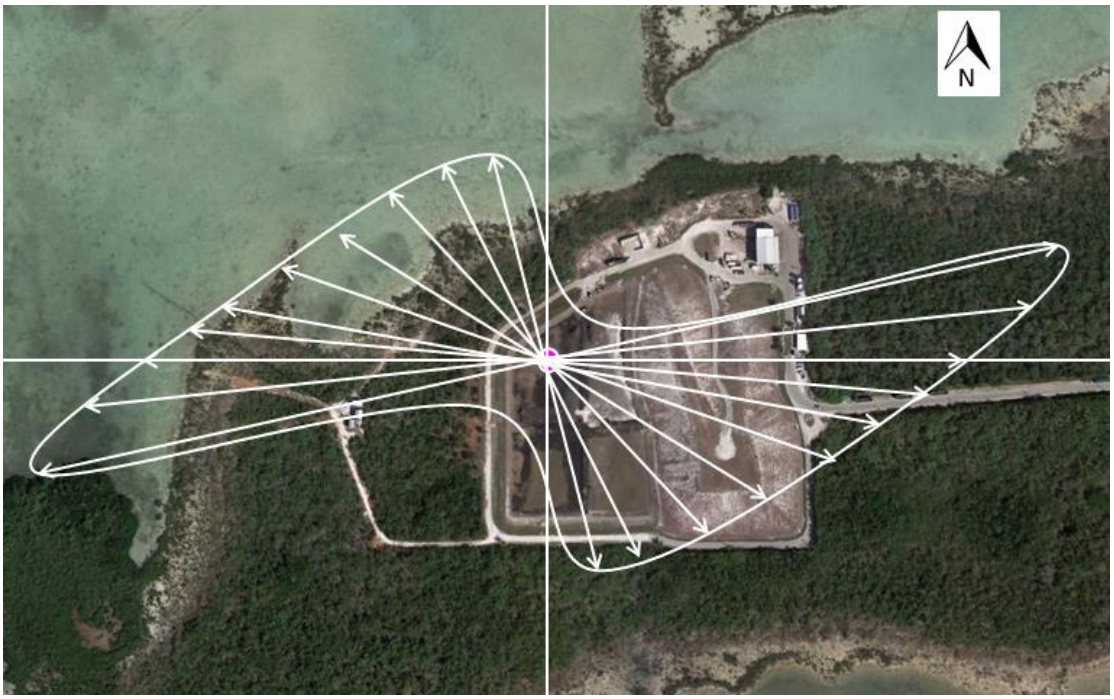


**Figure 27:** Hypothetical underground flow velocity field for water migrating from injection depth (80 ft to 120 ft) to shallow unconfined aquifer and surface waters.

# Conclusions

The Dye-tracer Injection Test described and documented above had one specific objective …"to either confirm or rule-out the existence of hydraulic connection between the shallow injection wells discharge and surface waters". We think that objective was achieved by documenting evidences that injected freshwater at the current injection depth of 80' to 120', and at the experimental rate of about 420 gal/min, will readily migrate upward and then laterally to the unconfined shallow aquifer and eventually to surface waters.

Two lines of evidence, support this conclusion, first is the physical evidence derived from the Freshwater Injection Test with the appearance of massive bubbling of displaced air coming from underground once injection began. These air bubbles are thought to be driven by ascending injected freshwater. But the most compelling evidence of connection was the venting of muddy freshwater from the bottom of a puddle next to the injection well. Those venting springs were necessarily connected to a high hydraulic head, above ground level, and disconnected to tidal fluctuations at the time of occurrence.

The second line of evidence comes from physical-chemical information, the appearance of dye at concentrations which were statistically anomalous following dye-injection. The estimated underground flow velocities reached very high values (up to 23 meters per hour or about 75 ft per hour), indicating the existence of a system controlled by large solution features an not inter-grain porosity. Results are similar to those found by other researchers elsewhere in the Florida Keys (Ref?).

# References


Böhlke, J.K., L.N. Plummer, E. Busenberg, T.B. Coplen, E.A. Shinn, P. Schlosser Origins, 1999. Residence Times, and Nutrient Sources of Marine Ground Water Beneath the Florida Keys and Nearby Offshore Areas. U.S. GEOLOGICAL SURVEY Open-File Report 99-181. P 2-4

Brinkmann, R. and Reeder, P., 1994, The influence of sea-level change and geologic structure on cave development in west-central Florida: Physical Geography, v.16. no.1, p. 52-61.

Coniglio, M. and Harrison, R.S., 1983a. Facies and diagenesis of Late Pleistocene carbonates from Big Pine Key, Florida. Bull. Can. Petrol. Geol., 31: 135-147.

Coniglio, M. and Harrison, R.S., 1983b. Holocene and Pleistocene caliche from Big Pine Key, Florida. Bull. Can. Petrol. Geol., 31: 3-13.

Cunningham, Kevin J., Donald F. McNeill, Laura A. Guertin, Paul F. Ciesielski, Thomas M. Scott and Laurent de Verteuil. 1998. New Tertiary stratigraphy for the Florida Keys and southern peninsula of Florida. Geological Society of America Bulletin, vol. 110, no. 2, pp. 231-258.

EPA. 2003. U.S. Environmental Protection Agency (EPA). (2003)Tracer-Test Planning Using the Efficient Hydrologic Tracer-Test Design (EHTD) Program. National Center for Environmental Assessment, Washington, DC; EPA/600/R-03/034. Available from: National Technical Information Service, VA; PB2003-103271, and <http://www.epa.gov/ncea>.

Hoffmeister, J.E. and H. G Multer. 1968. Geology and Origin of the Florida Keys. Geological Society of America Bulletin 1968; 79, no. 11; 1487-1502

Johns, G., Leeworthy, V., Bell, F. and Bonn, M. 2001. Socioeconomic study of reefs in southeast Florida. Report by Hazen and Sawyer under contract to Broward County, Florida. Fishand Wildlife Conservation Commission andNOAA.225 pp

Paul J. H., Rose J. B., Brown J., Shinn E. A., Miller S. and Farrah S. R. (1995) Viral tracer studies indicate contamination of marine waters by sewage disposal practices in Key Largo, Florida. Appl. Environ. Microbiol.61,2230-2234.

Paul, J.H., J.B. Rose, S.C. Jiang, X. Zhou, P. Cochran, C. Kellogg, J.B. Kang, D. Griffin, S. Farrah and J. Lukasik. 1997. Evidence for groundwater and surface marine water contamination by waste disposal wells in the Florida Keys.Wat. Res. Vol. 31, No. 6, pp.

Reich, C., E.A. Shinn, C. Hickey and A.B. Tihansky. 2001. Tidal and Meteorological Influences on Shallow Marine Groundwater Flow in the Upper Florida Keys in J. Porter and K.C Porter (Editors) The Everglades, Florida Bay,and Coral reefs of the Florida Keys. An Ecosystem Handbook. CRC Press. 1022 p.

Shinn, E.A., C. Reich, D. Hickey and A.B. Tihansky. 1999a. Determination of Groundwater-Flow Direction and Rate Beneath Florida Bay, the Florida Keys and Reef Tract. http://sofia.usgs.gov/projects/index.php?project_url=grndwtr_flow Downloaded Oct 2014

Shinn, E.A., R.S. Reese and C.D. Reich. 1999b. Fate and Pathways of Injection-Well Effluent in the Florida Keys. http://sofia.usgs.gov/publications/ofr/94-276/index.html Downloaded Oct 2014

Tihansky, A.B., 1999, Sinkholes, west-central Florida—A link between surface water and ground water, i: Galloway, Devin, Jones, D.R., and Ingebritsen, S.E., 1999, Land Subsidence in the United States: U.S. Geological Survey,Circular 1182, p. 121-141.

Tihansky, A.B., and Trommer, J.T., 1994, Rapid ground-water movement and transport of nitrate within a karst aquifer system along the coast of west-central Florida [abs.]: Transactions, American Geophysical Union, v. 75,April 19, 1994, Supplement, p. 156.

USACE. 2010. Florida Keys Water Quality Improvements Program. Florida Keys Aqueduct Authority Cudjoe Regional Wastewater System, Monroe County, Florida. U.S. Corps of Engineers, 147 pp.

U.S. Environmental Protection Agency (EPA). (2003) *Tracer-Test Planning Using the Efficient Hydrologic Tracer-Test Design (EHTD) Program*. National Center for Environmental Assessment, Washington, DC; EPA/600/R-03/034. Available from: National Technical Information Service, VA; PB2003-103271, and <http://www.epa.gov/ncea>

White, W.A., 1970, The geomorphology of the Florida peninsula: Florida Bureau of Geology, Bulletin no. 51, 164 p.

# APPENDIX 1

# Appendix 1

## Data Summary Report

# Characterization and quantitative determination of fluorescent dye concentrations in surface and ground water samples by 3D-Fluorescence

APRIL 2015

Preliminary Working Draft

**Prepared by**

**FLORIDA INTERNATIONAL UNIVERSITY**
SOUTHEAST ENVIRONMENTAL RESEARCH CENTER
ENVIRONMENTAL ANALYSIS RESEARCH LABORATORY
3000 Northeast 151st Street
North Miami, FL 33181
USA

# Table of Contents


**Chapter 1 Introduction ..... 47**

1.1 Study Plan Objectives ..... 47

**Chapter 2 Experimental ..... 48**

2.1 Chemicals and Reagents ..... 48

2.2 Instrument and Supplies ..... 48

2.3 Standard preparation ..... 48

2.4 Analytical procedure ..... 48

2.5 Calibration curves ..... 50

2.6 QA/QC samples ..... 53

**Chapter 3 Study Results ..... 54**

3.1 Baseline measurements ..... 54

3.2 Observation and injection well measurements after injection ..... 56

3.3 Pond and lake measurements ..... 57

**Chapter 4 Conclusions ..... 59**

## Figures

Figure 1 3D-EEMs of the fluorescence signature of Rhodamine (left) and Fluorescein (right) in de-ionized water

Figure 2 3D-EEMs of reclaimed water sample spiked with both fluorescein and rhodamine

Figure 3 Fluorescein calibration curve with different matrixes

Figure 4 Rhodamine calibration curve with different matrixes

Figure 5 Contour plots for a). OW1 b). OW2 c). OW4 d). OW5 e). IW1 f). IW4

Figure 6 Measured concentration of fluorescein for all samples acquired over time for a). OW1 b). OW2 c). OW4 d). OW5 e). IW1 f). IW4

Figure 7 Contour plots for pond (right) and lake (left)

Figure 8: Measured concentration of fluorescein for all samples in lake (top) and pond (bottom)

## Tables

Table 1 Water-Raman-peak signal-to-noise and emission calibration validation parameters

Table 2 Quinine Sulfate unit parameter

Table 3 Slope and $R^2$ for Fluorescein calibration curves

Table 4 Slope and $R^2$ for Rhodamine calibration curves

Table 5 Baseline average concentration of fluorescein and Rhodamine

**Acronyms and Abbreviations**

| | |
|---|---|
| DSR | data summary report |
| L | liter(s) |
| µg/L | microgram(s) per liter |
| µm | micrometers |
| mg | milligrams |
| mg/L | milligrams per liter (ppm) |
| mL | milliliters |
| µL | microliters |
| ppb | part per billion |
| RPD | relative percent difference |
| QC | quality control |
| QA | quality assurance |
| CK | check |

Chapter 1

# Introduction

## 1.1 Study Plan Objectives

The main objective of this study is to characterize two specific dyes (Fluorescein and Rhodamine) in water samples by utilizing excitation-emission fluorescence. Because of the high resolution sampling needed the instrument selected for the study was a HORIBA Aqualog spectrofluorometer which is capable of producing full range 3D Excitation-Emission matrixes (EEMs) in less than 2 minutes per sample. The first objective was to develop and validate an analytical method for the quantitative determination of the concentration of these particular dyes in environmental water samples representing different matrices (groundwater, surface waters and drinking water). The water samples to be analyzed were obtained from different wells surrounding a predetermined location that would be injected with a specific dye solution. Preliminary estimations required the robust detection of both dyes in all matrices at levels as low as 5 µg/L. The method was tested to assess the potential interferences of natural components and enough samples were analyzed to define the general background conditions pre-injection. The final objective was to successfully measure samples post-injection and assess the presence of the dyes at concentrations above the measured local or regional background.

Specific tasks included in this report:

- Characterization of dyes in water samples.
- Generation of an analytical method capable of determining the concentration of two specific dyes in multiple water sources that may be subject to potential natural interferences.
- Generation of local and regional baseline data.
- Assess the samples for the presence of the dye after injection.

Chapter 2

# Experimental

## 2.1 Chemicals and Reagents

- Tap water and de-ionized water.
- Uranine B (powder) by Pylam product company inc. (Tempe, AZ). CAS: 518-47-8
- Rhodamine (20%v/v) by Pylam product company inc. (Tempe, AZ).CAS: 37299-86-8

## 2.2 Instrument and Supplies

- Horiba-Scientific, Aqualog
- Aqualog V3.6 software
- 4.5 mL, 10 mm lightpath disposable plastic cuvette, Fisherbrand CAT No: 14-955-120
- 12, 40, 60 and 140 mL amber vials
- 10µl-10mL pipettes
- 10, 25, 50 and 100 mL volumetric flask

## 2.3 Standard preparation

The stock solution for Fluorescein was prepared by diluting approximately 20 mg of the reference standard (Uranine B) into 50 mL of the matrix water sample. The target concentration of the stock solution was approximately 400 ppm. An intermediate solution was prepared by series dilution of the stock in the matrix water sample to a concentration of 500 ppb. Initial calibration standards were prepared from the intermediate solution in volumes of 10 mL at the following concentrations: 0, 0.5, 1, 2, 4 and 8 ppb.

The stock solution of Rhodamine was prepared by dilution 500 µL of the reference standard (Rhodamine in liquid form, concentration= 200,000 mg/L) into 50 mL of the matrix water sample. The target concentration of the stock solution was 2,000 ppm. An intermediate solution was prepared by serial dilution of the stock solution (2000 ppm) in the matrix water sample to a concentration of 1000 ppb. Initial calibration standards were prepared from the intermediate solution in volumes of 10 mL at the following concentrations: 0, 0.4, 4.8, 9.7, 26.1 and 58.6 ppb.

## 2.4 Analytical procedure

### 2.4.1 Procedure summary

A Horiba Aqualog was utilized for the characterization of Fluorescein and Rhodamine by 3D-EEMs. The instrument was validated following procedures described in section 2.4.2 and an instrument method was developed (section 2.4.3). The characterization of Fluorescein and Rhodamine was performed by spiking a water sample with a known amount of Fluorescein and Rhodamine and generating the 3D-EEMS. Figure 1 shows the fluorescence signature of Rhodamine and Fluorescein in de-ionized water, respectively.

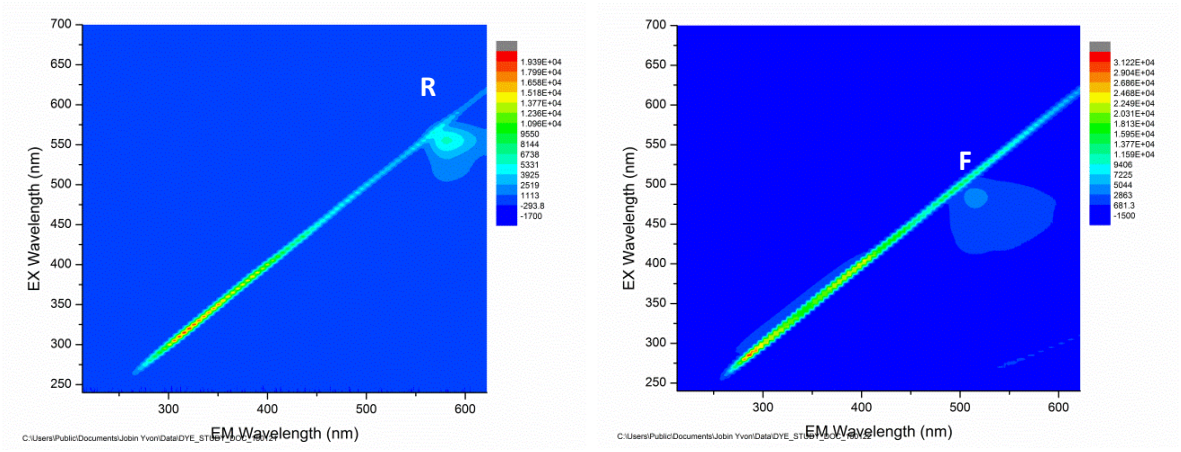


Figure 1 3D-EEMs of the fluorescence signature of Rhodamine (left) and Fluorescein (right) in de-ionized water. F and R represent the location of the Fluorescein and Rhodamine signals

From the 3D-EEMs, the maximun fluorescence intensity for Rhodamine was found at λex = 555nm and λem=581nm and for Fluorescein it was found at λex = 485nm and λem=514nm. In addition, a reclaimed water sample enriched in dissolved organic matter which also produces fluorescence was spiked with both dyes and figure 2 (left) shows the signature of the dyes did not interfere with the other fluorescence signature. An additional water sample with a large background fluorescence signal is shown (fig 2 right) spiked with Fluorescein to show distinction from background and dye.

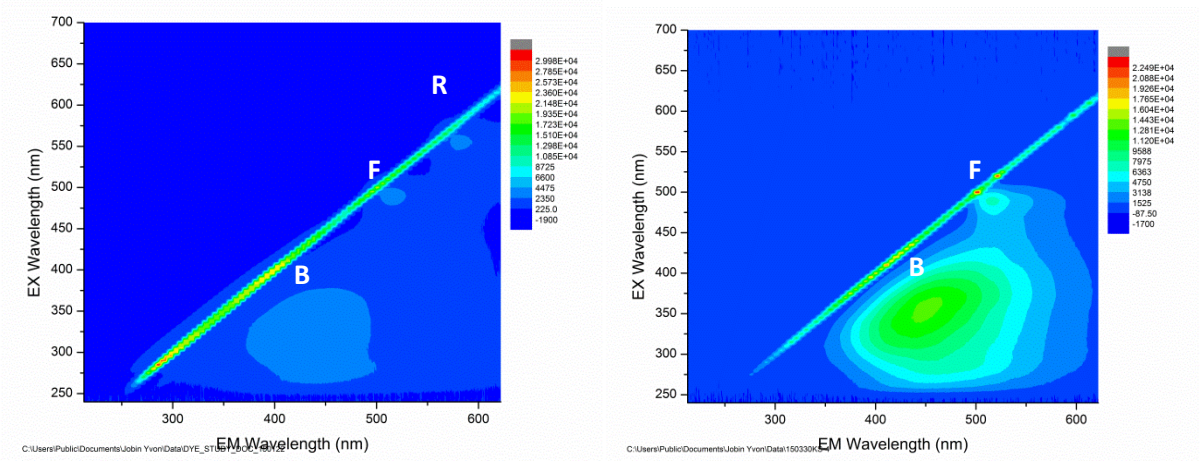


Figure 2 3D-EEMs of reclaimed water sample spiked with both Fluorescein and Rhodamine and matrix specific groundwater sample with large background signal spiked with Fluorescein (left). B is the background signal for the specific water matrix

Calibration curves were generated with both dyes by plotting the fluorescence response at the excitation-emission wavelength pair detailed earlier for each dye under different matrixes. Further detailed will be described in section 2.5 The sensitivity of the method was optimized and the linear range for the detection of fluorescein was set from 0.5 to 160 ppb and for Rhodamine it was set from 0.4 to 650 ppb. The calibration curves were initially verified by running an initial calibration verification standard with a known concentration of Fluorescein and Rhodamine from a different source of the calibration standards. For sample analysis, an analytical batch consisted of a laboratory fortified blank (LFB) to estimate the analytical

accuracy of the method, followed by a laboratory fortified matrix (LFM) sample to estimate the analytical accuracy in the presence of a representative matrix and a sample duplicate for analytical precision of the method. No sample preparation was required; samples were analyzed without sample manipulation. The sequence consisted of first an instrumental blank, followed by LFB, a random sample duplicate, LFM, samples separated per well (between 8-24 samples) and LFB. An LFM was prepared for each observation and injection well. The data was exported into excel and a macro was utilized to produce the fluorescence intensity at the designated excitation-emission wavelengths to be input into the calibration curve worksheet.

### 2.4.2 Instrument validation check

The Horiba-aqualog instrument was initially verified by performing a Water Raman SNR and emission calibration to examine the wavelength calibration of the CCD detector. The instrument was turned on and the lamp allowed to equilibrate for 15 minutes before use. After the software, Aqualog, was initiate the tab labelled as "collect" was selected followed by Aqualog Validation Tests-Water Raman SNR and Emission Calibration from the main window. The pre-set parameters and passing criteria are shown in table 1. This test utilizes triple-distilled, de-ionized water or HPLC-grade water for the analysis.

An additional validation check was performed which consisted of the analysis of a Quinine sulfate check solution in order to examine the accuracy of the wavelengths scanned. From the Aqualog Validation Tests window, the Quinine sulfate unit was selected. The parameters and passing criteria are shown in table 2. This test uses a solution of 1.28 x 10-6 mol/L of quinine sulfate in 0.105 mol/L of perchloric acid.

### 2.4.3 Instrument method

Three-dimensional excitation-emission matrix spectras (3D-EEMs) were generated directly from the Horiba—aqualog. The following instrument method was utilized for the generation of the 3D-EEMs.

Method Template: Aqualog-3DEEM_240_700_2

Data Description: Data Identifier: AQ3DXXX (this number should be obtained from the sequence logbook and be unique for each sample)
Comment: Name of the sample and description

Integration Time: 1 (s)
Accumulations: 1
Blank/Sample Setup: Sample Only
Wavelength Settings: Excitation Wavelength
High (nm): 700 Low (nm): 240
Increment (nm): 5
Emission Coverage: 212.90- 622.28 (nm)
Increment (nm): 0.82 nm (2 pixels)
CCD Gain: High

## 2.5 Calibration curves

A six point calibration curve for Fluorescein was generated based on the fluorescence intensity value at a specific $\lambda ex$ = 485nm and $\lambda em$=514nm in order to create a linear regression plot. The acceptable criterion for the calibration

curve was a linear fit that had an $R^2$>0.99. Calibration standards were generated under different matrixes to determine any matrix effects on the calibration curve. The matrixes consisted of tap water, pond water, observation well 2 (OW2), observation well 4(OW4) and observation well5 (OW5) sample waters. Figure 3 shows the calibration curves. Table 3 shows the slope of each curve and the $R^2$ value. No significant difference on linear fit and slope arose from matrix; therefore calibration curve with tap water was utilized for all sample analysis.

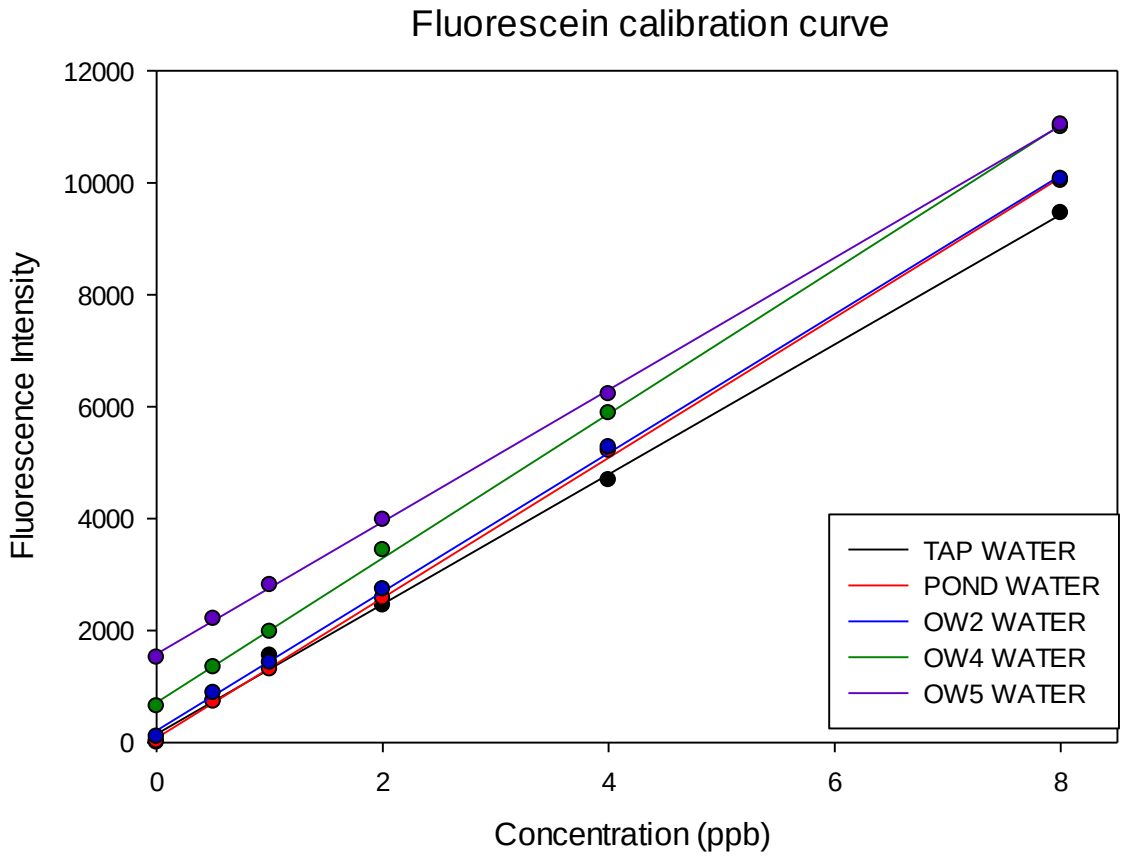


Figure 3 Fluorescein calibration curve with different matrixes

Table 3: Slope and $R^2$ for Fluorescein calibration curves

| Matrix | Slope of Linear fit | $R^2$ |
|---|---|---|
| TAP | 1160 | 0.9985 |
| POND | 1252 | 0.9997 |
| OW2 | 1240 | 0.9995 |
| OW4 | 1289 | 0.9996 |
| OW5 | 1180 | 0.9997 |

A six point calibration curve was also generated for Rhodamine based on the fluorescence intensity value at a specific λex = 555nm and λem=581nm in order to create a linear regression plot. Figure 4 shows the calibration

curves. Table 4 shows the slope of each curve and the $R^2$ value. No significant difference on linear fit and slope arose from matrix; therefore calibration curve with de-ionized water was utilized for all sample analysis.

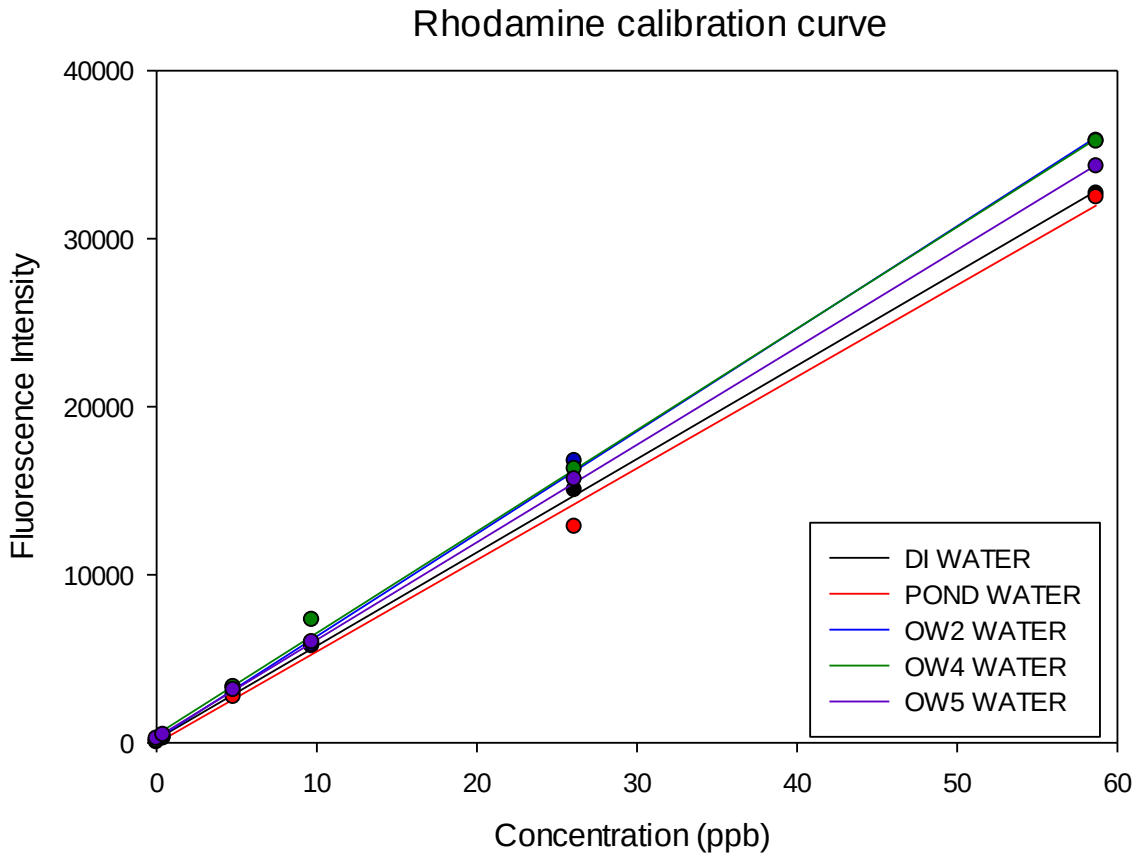


Figure 4 Rhodamine calibration curve with different matrixes

Table 3: Slope and $R^2$ for Rhodamine calibration curves

| Matrix | Slope of Linear fit | $R^2$ |
|---|---|---|
| DI | 556 | 0.9997 |
| POND | 545 | 0.9968 |
| OW2 | 611 | 0.9994 |
| OW4 | 604 | 0.9987 |
| OW5 | 581 | 0.9999 |

## 2.6 QA/QC samples

In order to verify the calibration curve, the following measurements were performed.

Initial verification calibration (ICVS)

A 4 and 30 ppb solution was prepared from a 400 ppb working solution standard from a different source of the calibration curve, Turner Design, for Fluorescein and Rhodamine, respectively. Since inactive ingredients in the Fluorescein standard could not be taken into account, the measured concentration for the 4 ppb fluorescein ICVS resulted in a 7 ppb value (55% RPD) the verification was corrected for bias deviations were assessed from the 7 ppb value. For Rhodamine, the measured concentration for the 30 ppb Rhodamine ICVS was 22 which resulted in 30% RPD so no correction for bias was applied.

Laboratory fortified blank (LFB)

A LFB was prepared daily at a concentration of 5 ppb and ran before an analytical batch and/or between 15-20 samples. The measured concentration did not deviate more than 25% RPD of the fortified value. The average % RPD for all the batches ran was calculated to be 8.73%. See appendix A for calculated values of all measured LFBs.

Laboratory Fortified Matrix (LFM)

An LFM was used to estimate analytical accuracy in the presence of a representative matrix. LFMs were generated for each of the wells sampled (IW4, IW1, OW2, OW4 and OW5) for each check points (CK01-12). A random sample was chosen and fortified with a matrix fortification solution to a concentration of 5 ppb. The acceptable LFM criterion was set as 70-130 % recovery. The average % recovery for all the batches ran was calculated to be 95.4 %. See appendix B for calculated values of all measured LFMs.

Duplicate analysis (DUP)

A sample duplicate was used to demonstrate sample homogeneity and analytical precision in the presence of a representative matrix. Duplicate analysis did not deviate more than 30% RPD from the original sample for the majority of the samples. Four out of 87 sample duplicates were more than 30% RPD. The average % RPD for all the batches ran was calculated to be 8.12%. See appendix C for calculated values of all measured sample duplicates.

Chapter 3

# Study Results

## 3.1 Baseline measurements

Before the introduction of the dye into the groundwater, the injection (IW) and observation (OW) wells were screened to obtain background concentrations of both fluorescein and rhodamine at different times. Pre-injection measurements consisted of ck01 to ck03.Table 5 shown below shows the samples collected at three different check points with the average ± one standard deviation for concentration of both Fluorescein and Rhodamine, respectively.

Table 5: Baseline average concentration of Fluorescein and Rhodamine

| Collection site | Samples collected | Average concentration of fluorescein (ppb) | Average concentration of rhodamine (ppb) |
|---|---|---|---|
| OW1 | CK01- 2/21/15-2/22/15 (24 samples) | 0.448 ± 0.0164 | 0.131 ± 0.0364 |
| | CK02- 2/22/15-2/24/15 (24 samples) | | |
| | CK03- 3/3/15 (14 samples) | | |
| OW2 | CK01- 2/20/15-2/21/15 (24 samples) | 0.105 ± 0.0094 | 0.0331 ± 0.00287 |
| | CK02- 2/22/15-2/24/15 (23 samples) | | |
| | CK03- 3/3/15 (15 samples) | | |
| OW4 | CK01- 2/20/15-2/21/15 (24 samples) | 0.495 ± 0.0516 | 0.123 ± 0.044 |
| | CK02- 2/21/15-2/23/15 (24 samples) | | |
| | CK03- 3/3/15 (15 samples) | | |
| OW5 | CK01- 2/20/15-2/21/15 (24 samples) | 1.198 ± 0.124 | 0.331 ± 0.060 |
| | CK02- 2/21/15-2/23/15 (24 samples) | | |
| | CK03- 2/24/15, 3/3/15 (15 samples) | | |
| IW1 | CK01- 2/21/15-2/22/15 (24 samples) | 0.790 ± 0.00958 | 0.0306 ± 0.0307 |
| | CK02- 2/22/15-2/24/15 (24 samples) | | |
| | CK03- 3/3/15 (14 samples) | | |
| IW4 | CK01-2/22/15 (2 samples) | 0.0694 ± 0.0272 | 0.0415 ± 0.0325 |
| | CK02- 2/22/15-2/25/15 (17 samples) | | |
| | CK03- 3/3/15 (14 samples) | | |

The following shows the contour plots for the analysis of water samples from the injection and observation wells before injection of the dye.

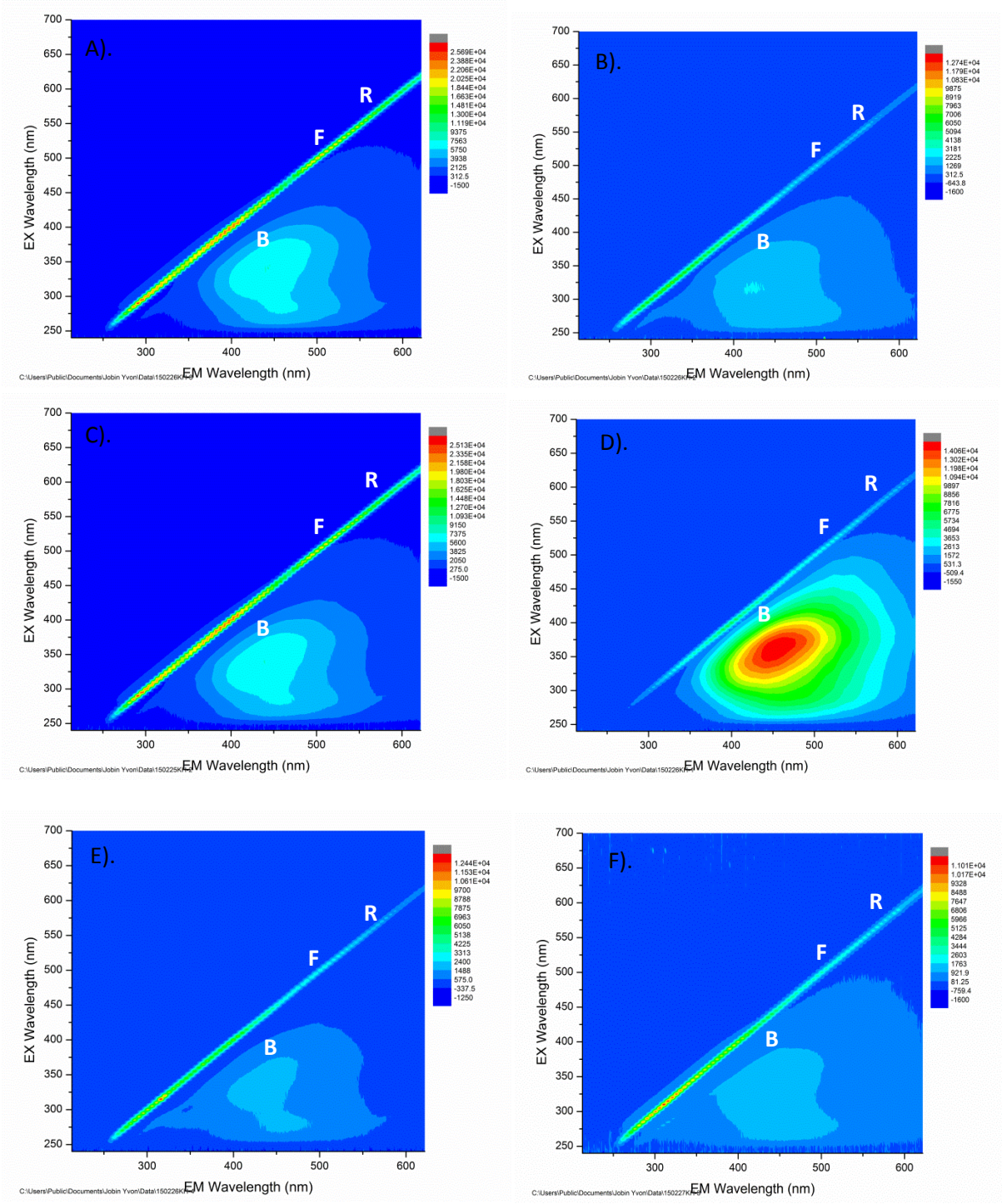


Figure 5 Contour plots for a). OW1 b). OW2 c). OW4 d). OW5 e). IW1 f). IW4. F and R represent the location of the Fluorescein and Rhodamine signals when present. B is the background signal for the specific water matrix.

## 3.2 Observation and injection well measurements after injection

Samples from ck04 to ck12 were screened for Fluorescein at each of the observation and injection wells. See appendix D for description of samples, collection and analysis time. Concentrations of Fluorescein were plotted for each sample processed for each well and the solid lines indicate the background baseline concentration and dash lines correspond to ± 1 SD. Figure 6 shows these plots.

A).

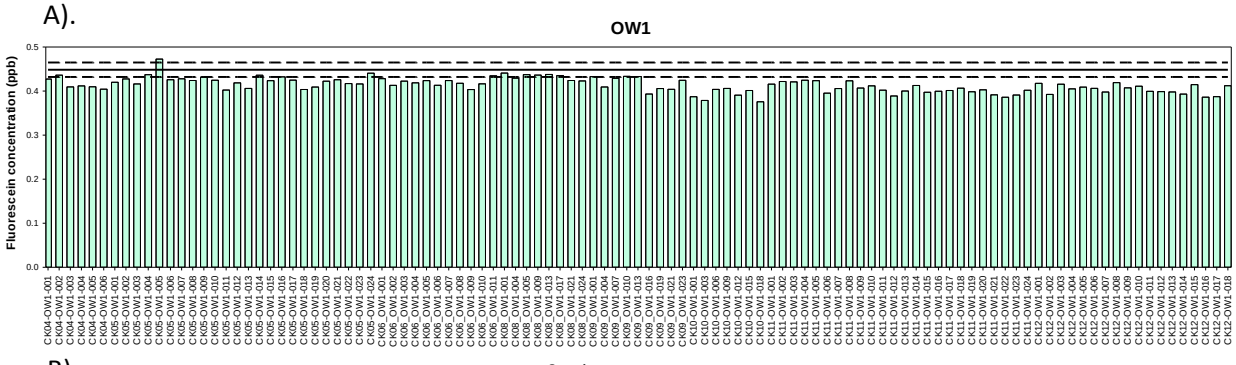


B).

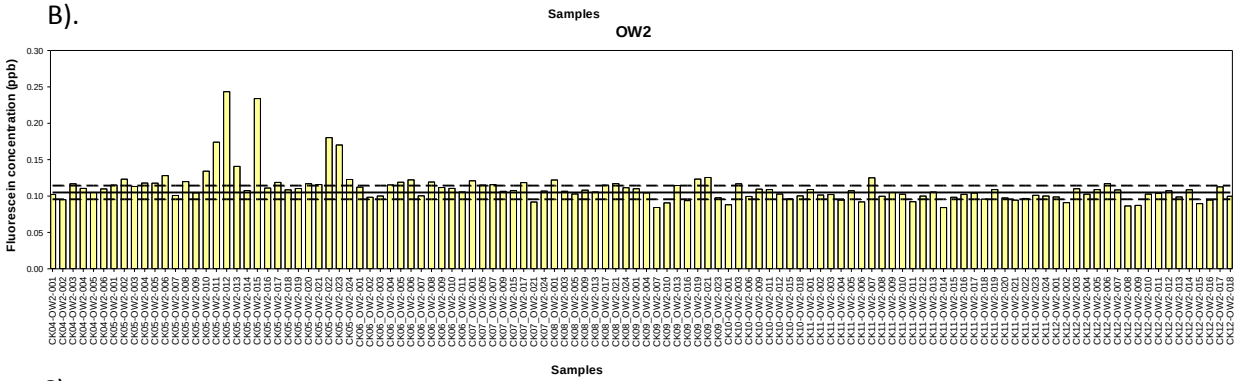


C).

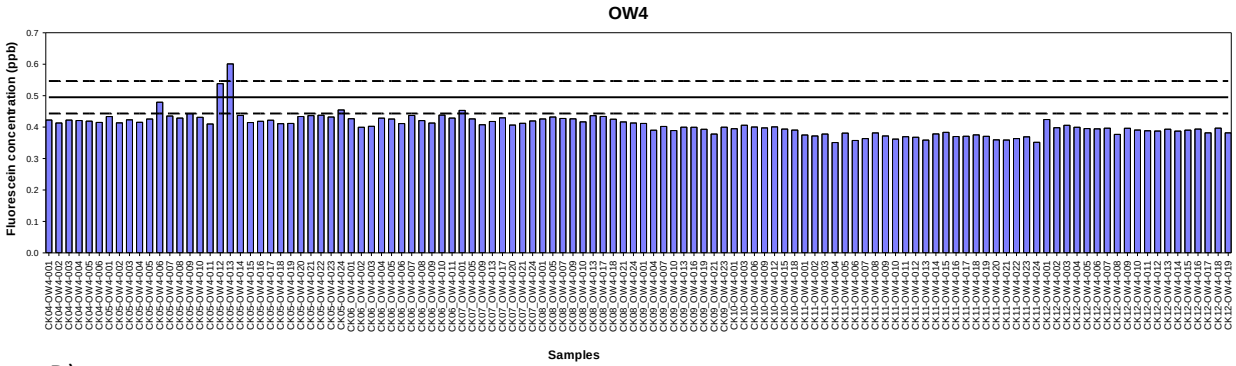


D).

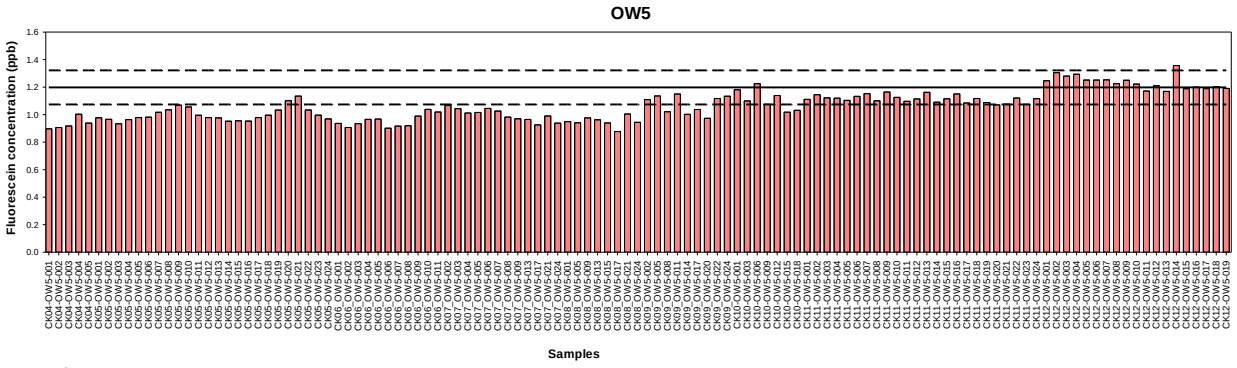


E).

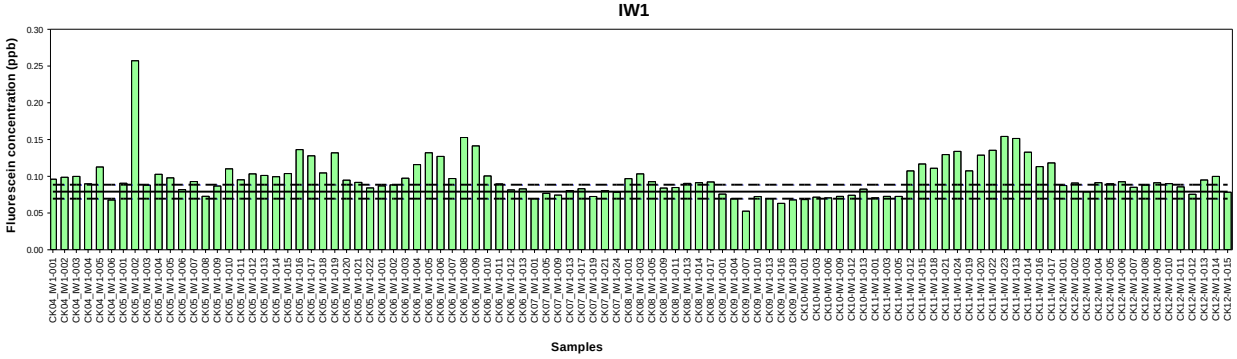


F).

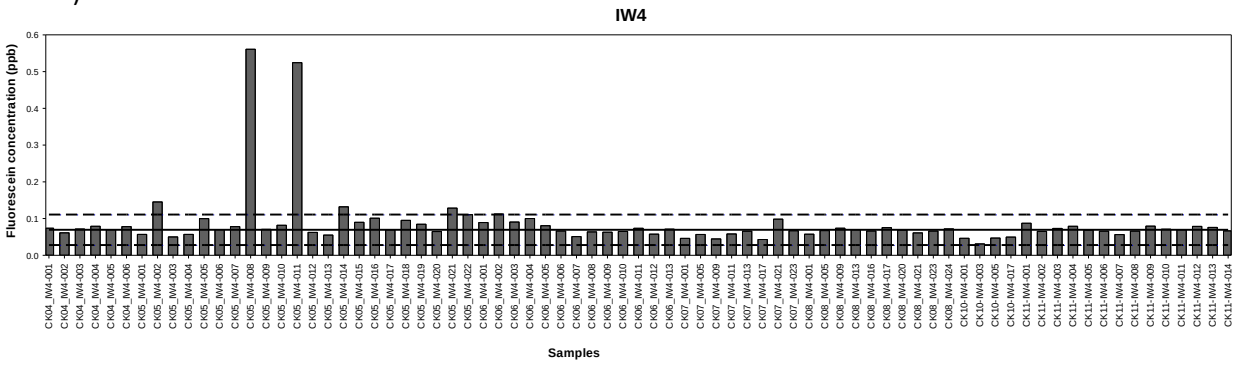


Figure 6 Measured concentration of Fluorescein for all samples acquired over time for a). OW1 b). OW2 c). OW4 d). OW5 e). IW1 f). IW4

No significant difference is observed between the measured concentration values for Fluorescein and the baseline for OW1, OW2 and OW4. A slight increase over time in concentration of Fluorescein is observed for OW5 but the concentrations are below the upper limit of the baseline. A slight increase in concentration of fluorescein is observed for IW1 at ck11 but declines at ck12.

## 3.3 Pond and lake measurements

Samples were also collected from the pond and lake at different locations and screened for Fluorescein after the injection period. Figure 7 shows an example of contour plots for both pond and lake, respectively.

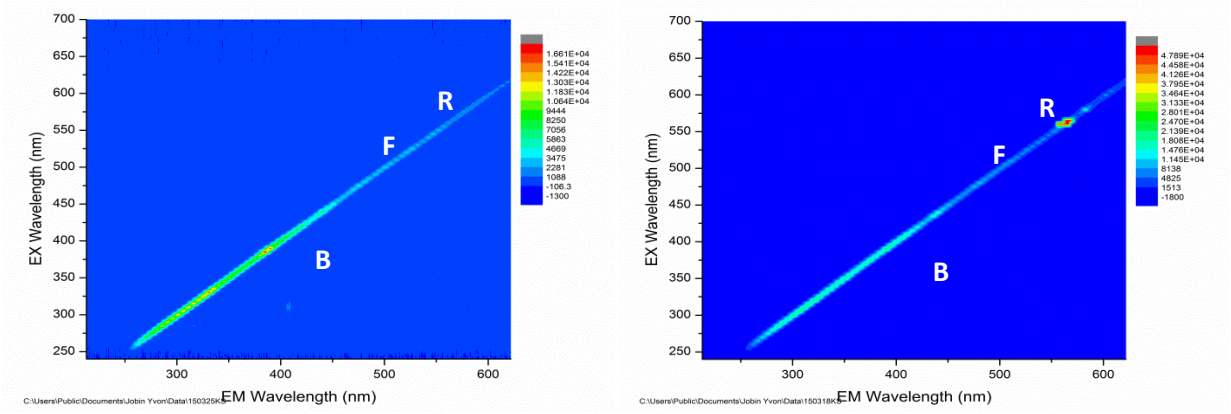


Figure 7 Contour plots for pond (right) and lake (left)

Figure 8 shows the Fluorescein concentrations plotted for the all samples collected over time from the lake and pond, respectively. Fluorescein concentrations from both the lake and the pond remained low throughout time.

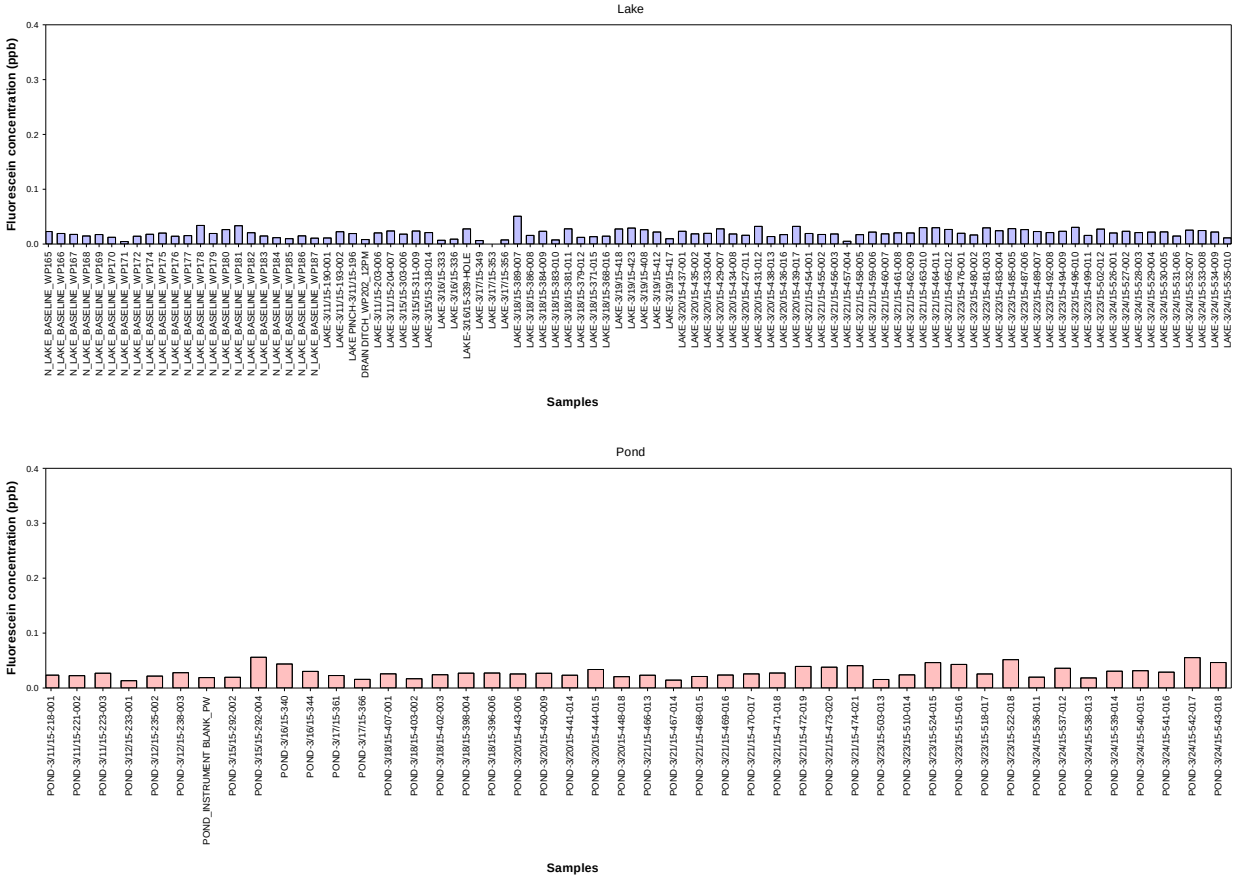


Figure 8 Measured concentration of Fluorescein for all samples in lake (top) and pond (bottom)

Chapter 4

# Conclusions

A method for the characterization and quantitative determination of Fluorescein and Rhodamine dye concentration was developed validated and employed for analysis of 1100 water samples types representing very different matrices. Baseline concentrations for the dyes were acquired at three different time points for the observation and injection wells. Fluorescein was monitored after injection in each of the wells and no appreciable changes in Fluorescein concentration trends observed.

Table 1: Water-Raman-peak signal-to-noise and emission calibration validation parameters

| | |
|---|---|
| Integration Time: | 30 (s) |
| Accumulations: | 1 |
| Blank/Sample Setup: | Sample only |
| Wavelength Settings: | Excitation Wavelength Park (nm) 350 |
| | Emission Coverage 210.07-619.62 (nm) |
| | Increment (nm) 0.82 nm (2 pixel) |

Passing criteria consist of the following:

Raman peak wavelength (nm): 397 ± 1 nm

Signal-Noise Ratio (SNR): > 20000

Table 2: Quinine Sulfate unit parameter

| | |
|---|---|
| Integration Time: | 0.1 (s) |
| Accumulations: | 1 |
| Blank/Sample Setup: | Sample and Blank |
| Wavelength Settings: | Excitation Wavelength Park (nm) 347.5 |
| | Emission Coverage 210.07- 619.62 (nm) |
| | Increment (nm) 0.41 nm (1 pixel) |

Passing criteria consist of the following:

%T > 96.5
Intensity of emission at 450nm counts observed: 1000-1400

# Appendix

A: See document QC_Aqualog_LFB_data

B: See document QC_Aqualog_LFM_data

C: See document QC_Aqualog_SDUP_data

D: See document Aqualog_alldata_worksheet

E: See document Aqualog_2015 logbook

F:See document Aqualog_uranine & rhodamine calibration curve